Bacillus subtilis utilizes decarboxylated S-adenosylmethionine for the biosynthesis of tandem aminopropylated microcin C, a potent inhibitor of bacterial aspartyl-tRNA synthetase

Alexey Kulikovsky, Eldar Yagmurov, Anastasiia Grigoreva, Aleksandr Popov, Konstantin Severinov, Satish Nair, Guy Lippens, Marina Serebryakova, Sergei Borukhov, Svetlana Dubiley

Bacillus subtilis utilizes decarboxylated S-adenosylmethionine for the biosynthesis of tandem aminopropylated microcin C, a potent inhibitor of bacterial aspartyl-tRNA synthetase

Alexey Kulikovsky[1], Eldar Yagmurov[1], Anastasiia Grigoreva[1], Aleksandr Popov[2,3], Konstantin Severinov[1], Satish K. Nair[4,5,6], Guy Lippens[7], Marina Serebryakova[8], Sergei Borukhov[9,]*, Svetlana Dubiley[7,]*

[1]Institute of Gene Biology, Russian Academy of Science, Moscow 119334, Russia

[2]RIKEN Center for Biosystems Dynamics Research, 1-7-22 Suehiro-cho, Tsurumi-ku, Yokohama 230-0045, Japan

[3]3Graduate School of Medical Life Science, Yokohama City University, Yokohama, Kanagawa 230-0045, Japan

[4]Department of Biochemistry, [5]Carl R. Woese Institute for Genomic Biology, [6]Center for Biophysics and Quantitative Biology, University of Illinois, Urbana, IL 61801, USA

[7]Toulouse Biotechnology Institute, Toulouse 31400, France

[8]A.N. Belozersky Institute of Physicochemical Biology MSU, 119992 Moscow, Russia

[9]Department of Molecular Biology, Virtua Health College of Medicine and Life Sciences, Rowan University School of Osteopathic Medicine, Stratford, NJ08084-1501, USA

*Authors to whom correspondence should be addressed: borukhse@rowan.edu, svetlana.dubiley@gmail.com

ABSTRACT

The biosynthetic pathways of natural products involve unusual biochemical reactions catalyzed by unique enzymes. Aminopropylation, though apparently simple, is an extremely rare modification outside polyamine biosynthesis. The canonical pathway used in the biosynthesis of peptide-adenylate antibiotic microcin C of *E. coli* (*Eco*-McC) entails alkylation by S-adenosyl-methionine-derived 3-amino-3-carboxypropyl group of the adenylate moiety and subsequent decarboxylation to yield bioactive aminopropylated compound. Here, we report the structure and biosynthesis of a new member of the microcin C family of antibiotics, *Bsu*-McC, produced by *Bacillus subtilis* MG27, that employs an alternative aminopropylation pathway. Like *Eco*-McC, *Bsu*-McC consists of a peptide moiety that facilitates prodrug import into susceptible bacteria, and a warhead - a non-hydrolyzable modified isoasparaginyl-adenylate, which when released in the cytoplasm, binds aspartyl-tRNA synthetase (AspRS), inhibiting translation. In contrast to the *Eco*-McC, whose warhead carries a single aminopropyl group attached to the phosphate moiety of isoasparaginyl-adenylate, the warhead of *Bsu*-McC is decorated with a tandem of two aminopropyl groups. Our *in silico* docking of the *Bsu*-McC warhead to the AspRS-tRNA complex suggests that two aminopropyl groups form extended interactions with the enzyme and tRNA, stabilizing the enzyme-inhibitor complex. We show that tandem aminopropylation results in a 32-fold increase in the biological activity of peptidyl-adenylate. We also show that *B. subtilis* adopted an alternative pathway for aminopropylation in which two homologous 3-aminopropyltransferases utilize a decarboxylated S-adenosylmethionine as a substrate. Additionally, *Bsu*-McC biosynthesis alters the social behavior of the *B. subtilis* producer strain, resulting in a sharp decrease in the ability to form biofilms.

INTRODUCTION

Natural products comprise a treasure trove of unusual chemical structures and biochemical reactions that produce them. Ribosomally synthetized post-translationally modified peptides (RiPPs) constitute a vast superfamily of natural products that combine structurally and functionally diverse groups of compounds.[1] RiPPs play important roles in bacterial physiology, including the mediation of quorum-sensing signals,[2] induction of complex morphogenesis,[3] serving as metallophores,[4] enzyme cofactors,[5] etc. Many RIPPs have antimicrobial or antifungal activity,[6] making them prospective leads for future antibiotic development.

RiPPs are classified into several families depending on the type of post-translational modifications and the enzymes that introduce them.[1,7] Microcin C-like compounds (McCs) constitute a unique family of RiPP antibiotics modified with nucleotides.[7] A typical McC is a peptide nucleotide consisting of a short formylated peptide and an adenosine or, less commonly, modified cytosine monophosphate moiety linked to a C-terminal isoasparagine residue (*i*N) *via* an N-P phosphamide bond. The best-studied member of the family, microcin C from *Escherichia coli* (*Eco*-McC), is a peptide-adenylate that is active at submicromolar concentrations against Enterobacteria, including clinically relevant *E. coli*, *Salmonella*, *Shigella*, and some strains of *Klebsiella* and *Yersinia*.[8,9] McC acts *via* a rare Trojan horse mechanism (Figure 1A). The peptide part of McC is responsible for binding to conserved YejABEF oligopeptide transporter and efficient import into the target bacteria.[10] Once in the cytoplasm, the peptide part is deformylated by the peptide deformylase PDF and then digested by cellular aminopeptidases,[11] releasing the active warhead, an isoasparaginyl-adenylate, *p*McC. *p*McC is a non-hydrolyzable structural analog of aspartyl-adenylate, a transient intermediate of the $tRNA^{Asp}$ aminoacylation. The warhead binds aspartyl-tRNA synthetase (AspRS) and prevents aminoacylation of $tRNA^{Asp}$, thereby inhibiting translation and halting cell growth.[12]

A minimal biosynthetic gene cluster (BGC) sufficient for producing a bioactive peptidyl-adenylate comprises only three genes: *mccA*, encoding a peptide precursor; *mccB* and *mccC*, coding for the family-defining nucleotidyltransferase and a major facilitator superfamily (MFS) export pump, respectively.[13] MccB modifies the MccA precursor peptide in a two-step reaction (Figure 1B), resulting in the formation of a bioactive peptidyl-acyl-N-P-adenylate[14,15] or peptidyl-acyl-N-P-cytidylate.[9,16] Many *mcc* BGCs, including that of *E. coli*, acquired additional genes responsible for secondary post-translational modifications or self-immunity.[17] The

peptidyl-adenylate of *E. coli* is additionally decorated with a rare post-translational modification, an aminopropyl group attached to the phosphate moiety.[18] This modification is introduced by the sequential action of $MccD^{Eco}$, the S-adenosylmethionine-dependent 3-amino-3-carboxypropyltransferase (ACP transferase), and $MccE1^{Eco}$, the N-terminal decarboxylase domain of the bifunctional $MccE^{Eco}$ protein (Figure 1B).[19] The addition of the aminopropyl group increases the inhibitory activity of the peptidyl-nucleotide eight-fold,[19] thus constituting a functionally important secondary modification. Identification of new activity-enhancing modifications of RiPPs and characterization of their biosynthetic pathways provide invaluable tools for engineering new-to-nature molecules with desired properties.

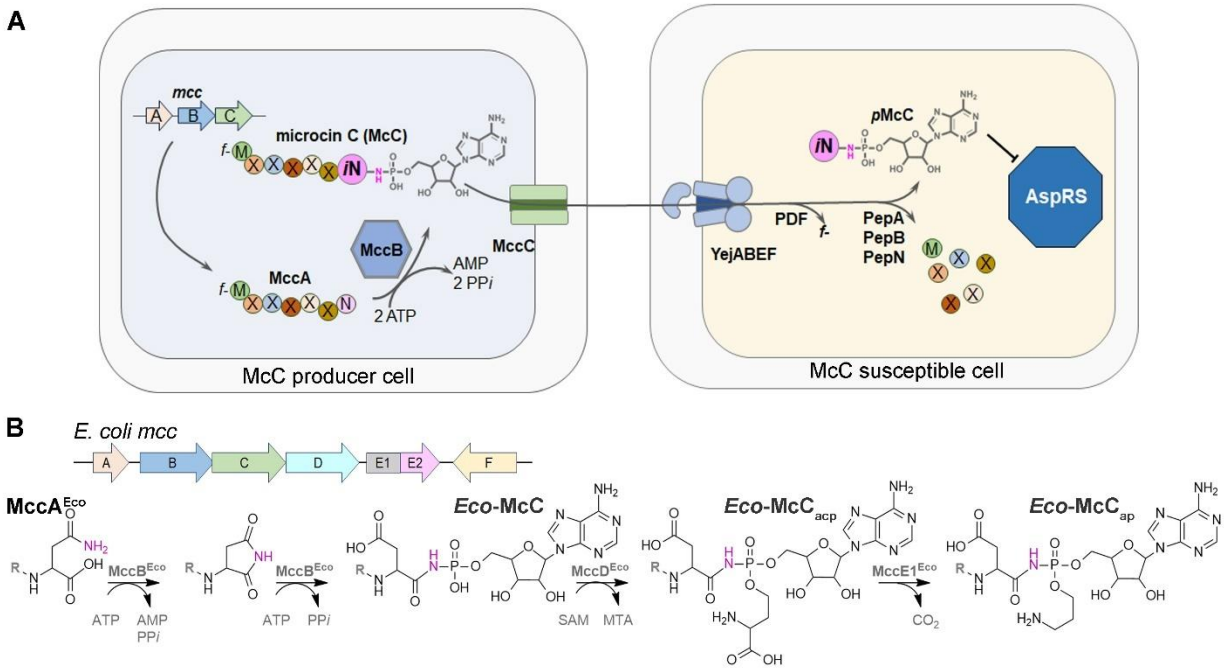

Figure 1. (A) Schematic diagram showing the mode of action of peptidyl-nucleotide antibiotics. (B) Organization of the biosynthetic gene cluster (top) and the key steps in the biosynthetic pathway of *E. coli* microcin C (bottom). $MccA^{Eco}$ - precursor peptide, $MccB^{Eco}$ – adenylyltransferase, $MccC^{Eco}$ - major facilitator superfamily export pump, $MccD^{Eco}$ – aminocarboxypropyl (ACP) transferase, $MccE1^{Eco}$ domain – decarboxylase, $MccE2^{Eco}$ domain – N-acetyltransferase, $MccF^{Eco}$ – L,D peptidase. $MccE2^{Eco}$ and $MccF^{Eco}$ are responsible for immunity function. YejABEF and PDF – cellular oligopeptide transporter and peptide deformylase, respectively. The isoasparaginyl-adenylate warhead of microcin C is designated *p*McC. R stands for the N-terminal part of $MccA^{Eco}$, MRTGNA. *Eco*-McC – adenylated $MccA^{Eco}$, *Eco*-McC_{acp} - adenylated $MccA^{Eco}$ decorated with 3-amino-3-carboxypropyl group, *Eco*-McC_{ap} – mature aminopropylated peptidyl-adenylate *E. coli*, MTA - 5'-methylthioadenosine.

Here, we report a new member of the McC-like RiPP family produced by *B. subtilis* MG27. The *B. subtilis* McC-like compound carries a unique secondary modification consisting of a tandem of two aminopropyl groups attached to the phosphate moiety of adenylate. Despite the structural similarity between *E. coli* and *B. subtilis* McCs, both microbes evolved alternative pathways for aminopropylation. In contrast to *E. coli* McC, *B. subtilis* McC aminopropylation modification requires decarboxylated S-adenosylmethionine as a substrate and is catalyzed by two aminopropyltransferases, MccM1^{Bsu} and MccM2^{Bsu}. We demonstrate that tandem aminopropylation results in a 32-fold increase in the bioactivity of peptidyl-adenylate. We also show that *Bsu*-McC biosynthesis causes hyperactive growth of *B. subtilis* MG27 and reduces its ability to form biofilm.

RESULTS

B. subtilis MG27 produces a peptidyl-nucleotide compound with a secondary modification at the phosphate group.

During a bioinformatic search for *mcc*-like biosynthetic gene clusters (BGCs) encoded in sequenced bacterial genomes we identified a gene for a putative MccB-like nucleotidyltransferase (MccB^{Bsu}) in the genome of the environmental strain of *Bacillus subtilis* MG27, a rhizosphere bacterium promoting grass growth and pathogen antagonism.[20] The *mccB*^{Bsu} is a part of a putative BGC that includes a gene encoding an MFS-like export pump (MccC^{Bsu}) and two genes coding for putative SAM-dependent enzymes, MccM1^{Bsu} and MccM2^{Bsu} (Figure 2A). A gene coding for RimL-like N-acetyltransferase MccE2^{Bsu} is located downstream of the putative *mcc*^{Bsu} BGC and transcribed in the opposite direction. MccE2^{Bsu} is homologous to the C-terminal domain of the *E. coli* MccE^{Eco}, [21] which allowed us to speculate that *mccE2*^{Bsu} could also be a part of the *mcc*^{Bsu} gene cluster. In the intergenic region between *mccB*^{Bsu} and *mccM2*^{Bsu}, we annotated a short open reading frame encoding a 22-amino-acid-long peptide with C-terminal asparagine residue (Figure 2A). We hypothesized that this peptide (MccA^{Bsu}) is a precursor for a McC-like compound.

To test if *B. subtilis* MG27 produces a biologically active McC-like compound, we analyzed the inhibitory effect of the *B. subtilis* MG27 spent medium on bacterial cell growth using a drop-diffusion assay on agar lawns. We did not detect growth inhibition of the laboratory strain of *B. subtilis* 168 or *E. coli* BL21, which precluded activity-based compound identification. The absence of antibiotic activity suggests that either *B. subtilis* MG27 does not produce the McC-

like compound under standard laboratory conditions, or the compound is not toxic to model microorganisms tested.

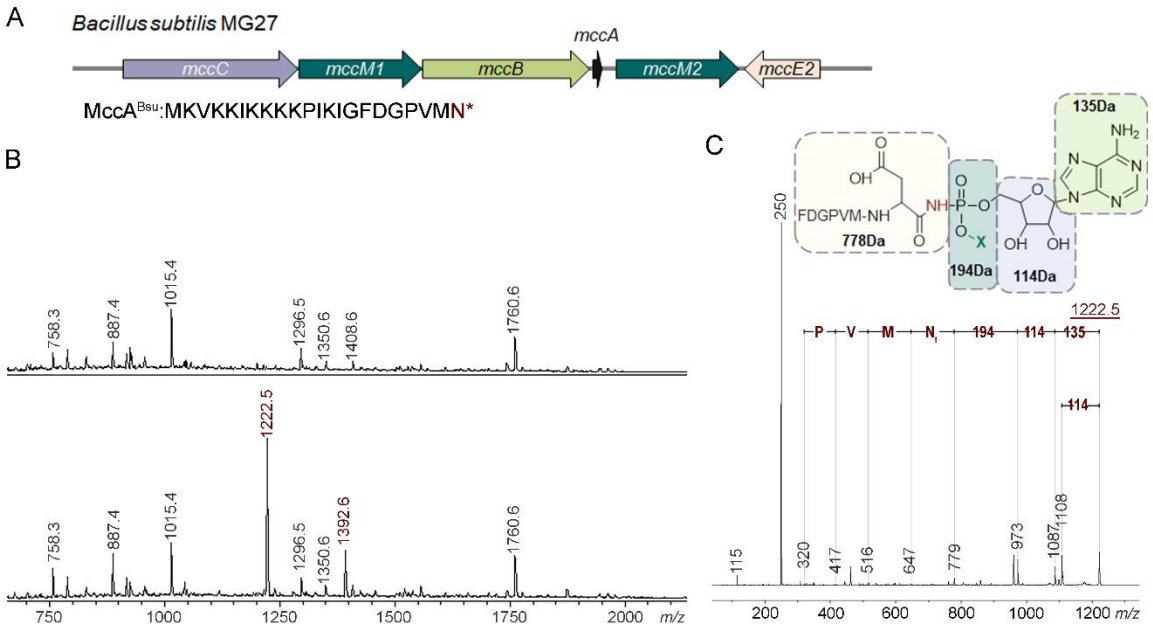

Figure 2. The *B. subtilis* MG27 *mcc* gene cluster (*mcc*^{Bsu}) and its products. (A) Architecture of the *mcc*^{Bsu} cluster and the sequence of predicted precursor peptide MccA^{Bsu}. Arrows representing genes are colored according to their functional annotations: *mccC*^{Bsu}, MFS transporter; *mccB*^{Bsu}, nucleotidyltransferase; *mccM1*^{Bsu} and *mccM2*^{Bsu}, SAM-dependent enzymes; *mccA*^{Bsu}, precursor peptide; *mccE2*, acetyltransferase. (B) MALDI-TOF MS analyses of the spent media of the control *B. subtilis* 168 carrying empty pHT01 control vector (upper panel) or pHT-*mccCM1BAM2*^{Bsu} plasmid (lower panel). $[M+H]^+$ ions related to the *mccCM1BAM2*^{Bsu} expression products are labeled in red. (C) MALDI-TOF/TOF MS analysis of the $[M+H]^+$=1222.5. $[M+H]^+$ product ions at *m/z* = 250 and *m/z* = 779 correspond to adenosine and FDGPVM*i*N peptide, respectively. The $[M+H]^+$ product ions at *m/z* = 1087 and *m/z* = 973 correspond to the modified peptides that lost adenosine and adenine moieties, respectively. The difference in 194 Da between $[M+H]^+$=779 and $[M+H]^+$=973 matches the phosphate residue (80 Da) bearing an unknown 114-Da modification designated with "X". The product ion $[M+H]^+$=1108, corresponding to the mature peptide that lost the 114-Da unknown modification, is complemented by $[M+H]^+$=115.

To construct an inducible *mcc*^{Bsu} expression system, we aimed to transfer the putative *mcc*^{Bsu} BGC into a heterologous host. However, first, we needed to determine whether the *mccE2*^{Bsu} gene, transcribed in the direction opposite to other cluster genes, is a part of *mcc*^{Bsu} BGC. Based on its homology to McC immunity acetyltransferase MccE2^{Eco},[21] which acetylates the amino group of the *Eco*-McC warhead, thus preventing its binding in the active center of aspartyl-tRNA synthetase, we hypothesized that MccE2^{Bsu} also functions as an immunity protein. We speculated that in the heterologous expression system, *mccE2*^{Bsu} could potentially rescue *E. coli* from the

inhibitory activity of *E. coli* peptide-adenylate (*Eco*-McC) or aminopropylated peptide-adenylate (*Eco*-McC$_{ap}$), the congeners of the putative *B. subtilis* McC. To test this hypothesis, *mccE2*^{Bsu} was cloned into the pBAD vector under an arabinose-inducible promoter, and the susceptibility of *E. coli* expressing predicted acetyltransferase to McC variants was assessed. As expected, the *mccE2*^{Bsu} expression effectively protected *E. coli* BL21 cells against both aminopropylated and non-aminopropylated forms of *Eco*-McC in an antibiotic drop-diffusion assay (Figure S1). These results demonstrate that similar to the C-terminal acetyltransferase domain of MccE^{Eco}, the single-domain MccE2^{Bsu} is responsible for the immunity function.

Next, we cloned the putative *mcc*^{Bsu} core cluster (*mccCM1BAM2*^{Bsu}) into the pHT01 vector for IPTG-inducible expression in the *B. subtilis* 168 laboratory strain. However, no inhibitory activity against *B. subtilis* 168 or *E. coli* BL21 was detected in the spent medium from *mcc*^{Bsu}-expressing *B. subtilis*. To confirm the production of the McC-like compound, we used MALDI-TOF MS analysis to compare the spent media from cultures of *B. subtilis* 168 strains carrying either the pHT-*mccCM1BAM2*^{Bsu} or the control empty pHT01 plasmid, both grown under inducing conditions. In the spent medium of *B. subtilis* 168 expressing *mcc*^{Bsu}, two mass ions, $[M+H]^+$=1222.5 and $[M+H]^+$=1392.6, which were absent in control, were detected (Figure 2B). MALDI-TOF/TOF MS analysis of the major mass ion $[M+H]^+$=1222.5 unambiguously identified the compound as an seven residue-long C-terminal part of the MccA^{Bsu} peptide modified with adenosine monophosphate carrying an additional 114-Da moiety on the phosphate group (Figure 2C). The $[M+H]^+$=1392.6 mass ion (Figure 2B) corresponds to the same modified peptide with an additional two-residue N-terminal extension. No mass ion matching the modified full-length (22-residue) MccA^{Bsu} was detected. When we compared the mass spectra of spent media from the *B. subtilis* cells harboring pHT-*mccCM1BAM2*^{Bsu} and the natural producer *B. subtilis* MG27, the same mass ions, $[M+H]^+$=1222.5 and $[M+H]^+$=1392.6, were identified in both samples (Figure S2) and no other MccA^{Bsu}-related mass ions detected. These results confirm that mature *B. subtilis* McC (*Bsu*-McC) is a modified C-terminal fragment of the precursor peptide, likely trimmed from the N-terminus by cellular peptidases before secretion, as seen in other RiPPs produced by *Bacilli*.[22]

B. subtilis peptidyl-adenylate is modified by two aminopropyl groups in a sequential two-step reaction.

To elucidate the structure of *Bsu*-McC, we first determined the mass of the compound purified from *B. subtilis* MG27 spent medium (Figure S3) using high-resolution mass spectrometry. The measured mass of the protonated compound (FDGPVM*i*N-AMP-X) is 1222.5081 (Figure 3A). The calculated monoisotopic mass of the protonated adenylated $MccA^{Bsu}$ fragment (FDGPVM*i*N-AMP, $C_{44}H_{63}N_{13}O_{17}PS$) is 1108.3923 Da. Assuming that the sought modification replaces the proton on the phosphate moiety, the mass difference of 114.1158 Da corresponds to the chemical formula $C_6H_{15}N_2$ (mass error 0.08 ppm).

Next, we performed a detailed NMR analysis. Before the measurements, we partially removed the peptide part of the *Bsu*-McC using a mixture of purified *E. coli* PepB, and PepN aminopeptidases[11] to simplify the spectra. This treatment yielded a partially digested peptide containing five C-terminal amino acid residues, GPVM*i*N (Figure S4). We first recorded spectra at 293 K of the partially processed *Bsu*-McC dissolved in a 90%/10% H_2O/D_2O solution at pH ~5. The 3 amino acids preceding the phospho-amide bond could be easily assigned based on homonuclear TOCSY and ROESY spectra (Figure S5, Table S1). When we analyzed the $^{1}H/^{13}C$ HSQC and $^{1}H/^{13}C$ HSQC-DIPSI spectra, we detected two different propyl groups in addition to the ribose ring and AMP adenine (Figure 3B, Figure S6, Table S1).

To identify the chemical group(s) attached to the phosphate moiety, we recorded J-resolved experiments with or without ^{31}P π pulse in the t1 evolution period. Only protons with a direct scalar coupling towards the ^{31}P nucleus should show a different multiplet structure in the two spectra.[23] The resulting spectra (Figure 3C, Table S1) allowed unambiguous identification of the propyl group linked to the phosphorous, with chemical shift values of 4.21 ppm/68.3 ppm for its α methylene group, 2.08/28.9 ppm for the central β methylene, and 3.15/47.4 ppm for the γ methylene group that is bound to the central nitrogen (Figure S6, Table S1). In the second propyl group, no proton showed any coupling to the ^{31}P. The chemical shifts of the protons in this propyl group perfectly matched the published chemical shift values for the spermine.[24] Thus, our data suggest the presence of the tandem aminopropyl group attached to the phosphate of the peptidyl-adenylate.

The phospho-amide proton and the secondary amine proton on the nitrogen atom separating both propyl groups were not visible in the spectra in water. To observe them, we lyophilized the

sample and dissolved it in 200 µL of DMSO-d6. Further acidification of this solution with 1 µL of concentrated (37%, 12 M) DCl revealed the phospho-amide group at 9.83 ppm for its proton and ^{15}N value of 117.6 ppm (Figure S7A, Table S1). The secondary amine proton showed up as a large signal that coupled to the protons of both propyl groups (Figure S7B, Table S1).

Altogether, analysis of the combined MS and NMR spectra allowed us to identify an unusual 3-((3-aminopropyl)amino)propyl group attached to the phosphate moiety of the peptidyl-adenylate (Figure 3D).

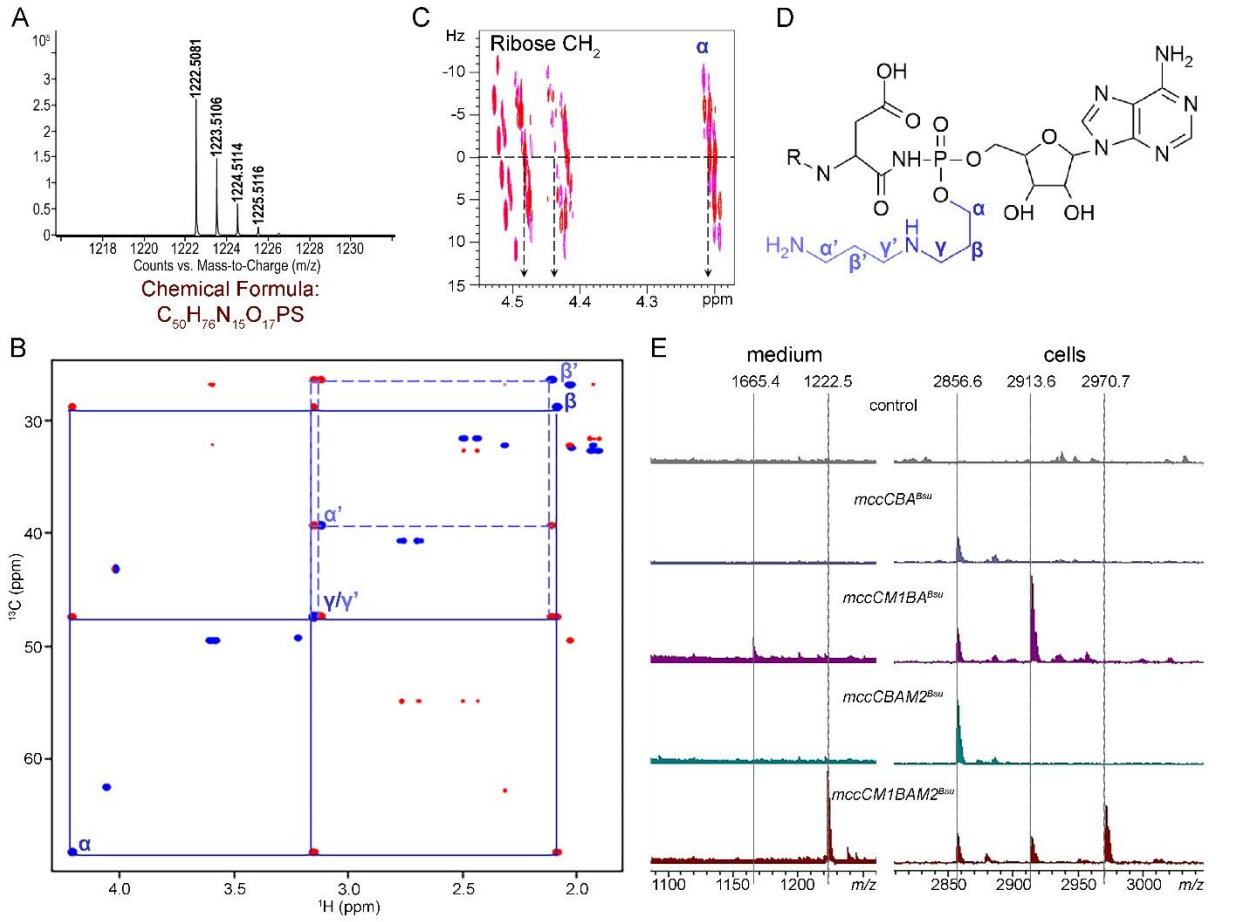

Figure 3. MccM1^{Bsu} and MccM2^{Bsu} catalyze the sequential addition of two aminopropyl groups on peptidyl-adenylate. (A) High-resolution mass-spectrum and chemical formula of *Bsu*-McC. (B) Two-dimensional ^{1}H - ^{13}C HSQC (blue), and HSQC-Dipsi (red) NMR spectra show the assignment of the two aminopropyl groups that decorate the phosphate group of the AMP moiety. (C) The overlay of two J-resolved spectra with (red) or without (magenta) recoupling of the ^{1}H, ^{31}P coupling constants identifies those protons with a direct scalar coupling constant to the ^{31}P. Dashed arrows point to the chemical shift values of the ^{31}P coupled ribose CH_2 protons and the α proton of the proximal propyl group, for which the two spectra are different. (D) Proposed chemical structure of *Bsu*-McC with numbering of the tandem aminopropyl atoms. R stands for the

peptidyl moiety FDGPVM. (E) MALDI-TOF MS analysis of spent media (left panel) and cell content (right panel) of *B. subtilis* 168 harboring plasmids with *mcc*^{Bsu} cluster variants and control vector. For detailed spectra analysis, see the text.

To uncover the mechanism of post-translational modification, we engineered a series of plasmids carrying the *mcc*^{Bsu} cluster with specific gene deletions and analyzed the resulting biosynthetic products by mass spectrometry. As shown in Figure 3E, the spent medium from the *B. subtilis* 168 cells expressing the minimal *mccCBA*^{Bsu} BGC contained no detectable mass ions corresponding to the peptidyl-adenylate. However, the MALDI-TOF MS analysis of the cells sample identified the product ion corresponding to the full-length precursor peptide decorated with adenylate ($[M+H]^+$=2856.6, Figures 3E and S8A). When putative methyltransferase gene *mccM1*^{Bsu} was added to the minimal *mccCBA*^{Bsu} cluster, new mass ions, $[M+H]^+$ at *m/z* 2913.6 and *m/z* 1665.4, were detected in the cells sample and the spent medium, respectively (Figure 3E). Subsequent MALDI-TOF/TOF MS analysis (Figure S8B) identified the $[M+H]^+$ at *m/z* 2913.6 as the adenylated MccA^{Bsu} modified with a 57-Da moiety attached to the phosphate. This modification matches the addition of a single aminopropyl group. The mass ion $[M+H]^+$ = 1665.4 corresponds to the N-terminally truncated seven-residue-long fragment of the same compound. No difference was detected between the mass spectra of *B. subtilis* cells carrying the minimal *mccCBA*^{Bsu} or extended *mccCBAM2*^{Bsu} BGCs (Figure 3E), indicating that peptidyl-adenylate cannot serve as a substrate for the MccM2^{Bsu}. Expression of the core *mcc*^{Bsu} BGC containing both putative methyltransferases (*mccCBAM1M2*^{Bsu}) resulted in the accumulation of the fully modified peptidyl-adenylate containing a tandem of two aminopropyl groups ($[M+H]^+$=2970.7, Figures 3E and S8C) within the cells. Although both biosynthetic intermediates, the peptidyl-adenylate and aminopropylated peptidyl-adenylate, were observed within the producing cells along with the fully modified compound, only mature *Bsu*-McC ($[M+H]^+$=1222.5) was detected in the spent medium (Figure 3E). Together, our data demonstrate that modification of MccA^{Bsu} proceeds in three consecutive steps: first, the MccB^{Bsu} nucleotidyltransferase adenylates the precursor peptide, next the MccM1^{Bsu} aminopropyltransferase installs the first aminopropyl group, followed by the final step of aminopropylation performed by MccM2^{Bsu} enzyme.

The biosynthesis of *Bsu*-McC hijacks the polyamine biosynthetic pathway.

Sequential installation of aminopropyl groups on the phosphate moiety of the adenylated MccA^{Bsu} precursor peptide resembles the aminopropylation pathway in the biosynthesis of *E. coli* McC.[19] Although, in contrast to *E. coli* (Figure 1B), *mcc*^{Bsu} BGC lacks gene(s) coding for a decarboxylase, hypothetically, an unknown cellular decarboxylase may perform the function of MccE1^{Eco}. However, in the presence of SAM, neither MccM1^{Bsu} nor MccM2^{Bsu} modified purified adenylated precursor MccA^{Bsu} (Figure S9) in an *in vitro* assay (Figures S10). Moreover, we never observed a mass ion corresponding to 3-carboxy-3-aminopropylated peptidyl-adenylate, the putative intermediate products of this reaction (Figure 1B and 3E, right panel), in samples prepared from whole cells. We therefore surmised that MccM1^{Bsu}/MccM2^{Bsu} may utilize decarboxylated SAM (dcSAM), an intermediate product of the spermidine biosynthetic pathway, as a source of the aminopropyl group.

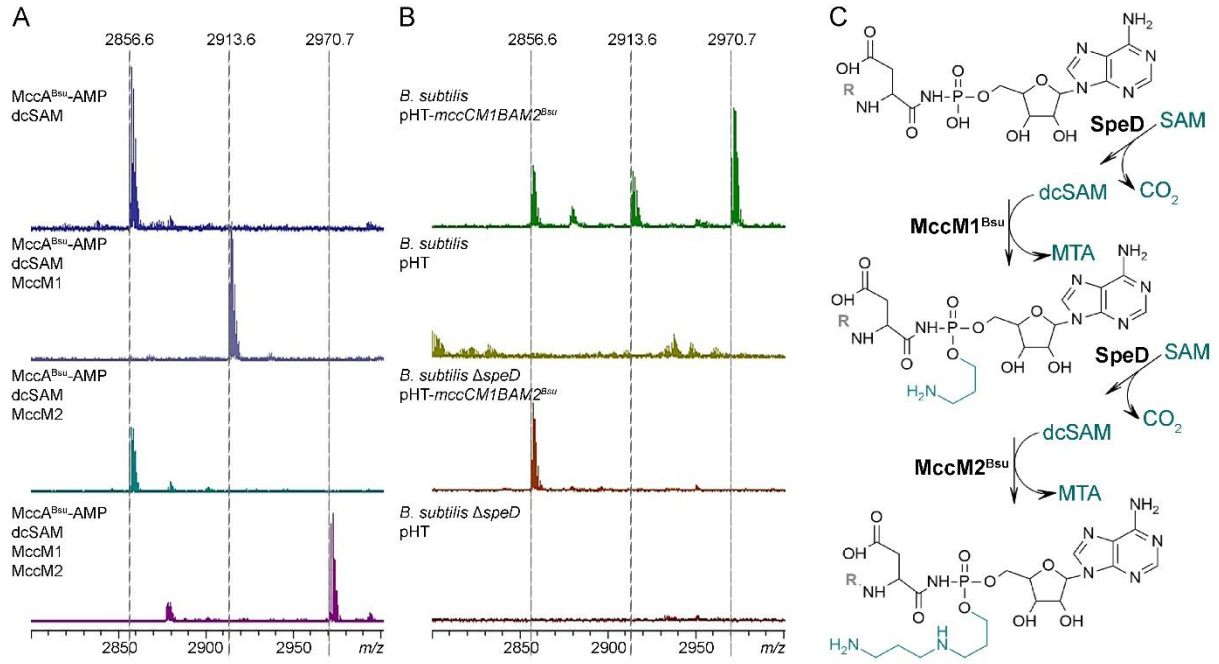

Figure 4. MccM1^{Bsu} and MccM2^{Bsu} use decarboxylated SAM as a substrate for aminopropylation. (A) MALDI-TOF MS analysis of *in vitro* aminopropylation reactions. MccM1^{Bsu} transfers the aminopropyl group from dcSAM to peptidyl-adenylate MccA^{Bsu}-AMP ([M+H]$^+$=2856.6). MccM2^{Bsu} converts aminopropylated peptidyl-adenylate ([M+H]$^+$=2913.6) into tandem aminopropylated form ([M+H]$^+$=2970.7) using dcSAM. (B) SpeD^{Bsu} activity is required for the maturation of *Bsu*-McC *in vivo*. MALDI-TOF MS analysis of *mcc*^{Bsu} products in wild-type and Δ*speD B. subtilis* genetic background. (C) Scheme of *B. subtilis* peptidyl-adenylate aminopropylation pathway. R stands for the N-terminal part of MccA^{Bsu}, MKVKKIKKKKPIKIGFDGPVM.

To test this hypothesis *in vitro*, we converted SAM into dcSAM using the purified housekeeping *E. coli* SAM decarboxylase SpeD (Figure S11) and added it as a substrate to the reaction mixture containing purified adenylated $MccA^{Bsu}$ (Figure S9) and $MccM1^{Bsu}$ and/or $MccM2^{Bsu}$ enzymes. The reaction was also supplemented with 5'-methylthioadenosine/S-adenosylhomocysteine nucleosidase Mtn^{Eco} to relieve potential product inhibition of aminopropyl/aminocarboxypropyltransferases.[19] Figure 4A shows that in the presence of dcSAM, $MccM1^{Bsu}$ converted adenylated $MccA^{Bsu}$ into the aminopropylated compound. In agreement with our *in vivo* experiments (Figure 3E), $MccM2^{Bsu}$ alone did not modify the adenylated precursor peptide in the presence of dcSAM. However, in the presence of $MccM1^{Bsu}$ and $MccM2^{Bsu}$, a compound with a mass matching the mature unprocessed *Bsu*-McC was observed (Figures 3E and 4A). To examine whether $MccM2^{Bsu}$ shares the same narrow specificity for dcSAM as $MccM1^{Bsu}$, we purified the product of the first aminopropylation reaction ($MccA^{Bsu}$-AMP-ap) catalyzed by $MccM1^{Bsu}$ and used it as a substrate in a second aminopropylation reaction with $MccM2^{Bsu}$ in the presence of either SAM or dcSAM. MALDI-TOF MS analysis revealed that $MccM2^{Bsu}$ modified the monoaminopropylated substrate only in the presence of dcSAM (Figure S12), confirming that the entire biosynthetic pathway relies on this unusual metabolite.

In *B. subtilis*, SpeD is the only enzyme able to decarboxylate SAM.[25] Therefore, to confirm the proposed biosynthetic pathway *in vivo*, we constructed the *B. subtilis* 168 *speD* deletion mutant and analyzed the McC-like compounds produced by this strain. As expected, the adenylated peptide was readily made in the *B. subtilis* cells lacking functional SpeD, but no aminopropylated species were detected (Figure 4B).

Combined, our *in vivo* and *in vitro* data show that $MccM1^{Bsu}$ and $MccM2^{Bsu}$ jointly modify the phosphate group of the peptidyl adenylate by sequentially adding two aminopropyl groups using dcSAM as a substrate (Figure 4C).

The presence of two aminopropyl groups increases the bioactivity of McC.

Purified *Bsu*-McC did not affect the growth of *B. subtilis* 168 and had only a minor inhibitory effect on the growth of *E. coli* BL21, even at 2 mM (Figure S13). The resistance of *B. subtilis* could be due to the absence of the YejABEF oligopeptide transporter[10] or the presence of genome-encoded S51 family peptidases MccG, which cleaves the carboxamide bond of

isoasparaginyl-adenylate, thus providing immunity to McC-like compounds.[26] However, the lack of *Bsu*-McC inhibitory effect on *E. coli* cells is puzzling. Theoretically, it could be caused by poor uptake of *Bsu*-McC by *E. coli* YejABEF, inefficient processing of the *Bsu*-McC peptide by *E. coli* cellular aminopeptidases, or weak binding to the cellular target.

To address this conundrum, we first performed *in silico* docking of tandem-aminopropylated isoasparagine-adenylate into the active site of AspRS using the crystal structure of the *E. coli* AspRS in complex with $tRNA^{Asp}$ and aspartyl-adenylate (PDB: 1C0A)[27] as a template for modeling. The docking model, generated using CB-Dock2[28] and further refined with Molsoft ICM-Pro 3.9, shows that without tRNA, the *Bsu*-McC warhead fits nicely into the enzyme's catalytic pocket without clashes with the polypeptide backbone or side chains (Figure 5A). The isoasparagine-adenylate moiety of *Bsu*-McC superimposes well with the natural substrate aspartyl-adenylate with a root mean square deviation (RMSD) = 0.48 Å, making similar hydrogen bonds, polar, and van der Waals contacts with AspRS active site residues (Figure 5A-C). The tandem aminopropyl groups of the *Bsu*-McC warhead contribute to binding by interacting with several polar and hydrophobic side chains of AspRS residues. Of these, the most prominent contact is by the secondary amine of the proximal aminopropyl group, which is predicted to make a hydrogen bond with the carboxylic group of E482 (Figure 5B). The more flexible distal aminopropyl group makes polar contacts via its primary amine with the carboxylic group of E437 and carbonyl of H448, while the propyl group makes hydrophobic interactions with the side chain of M447 (Figure 5B).

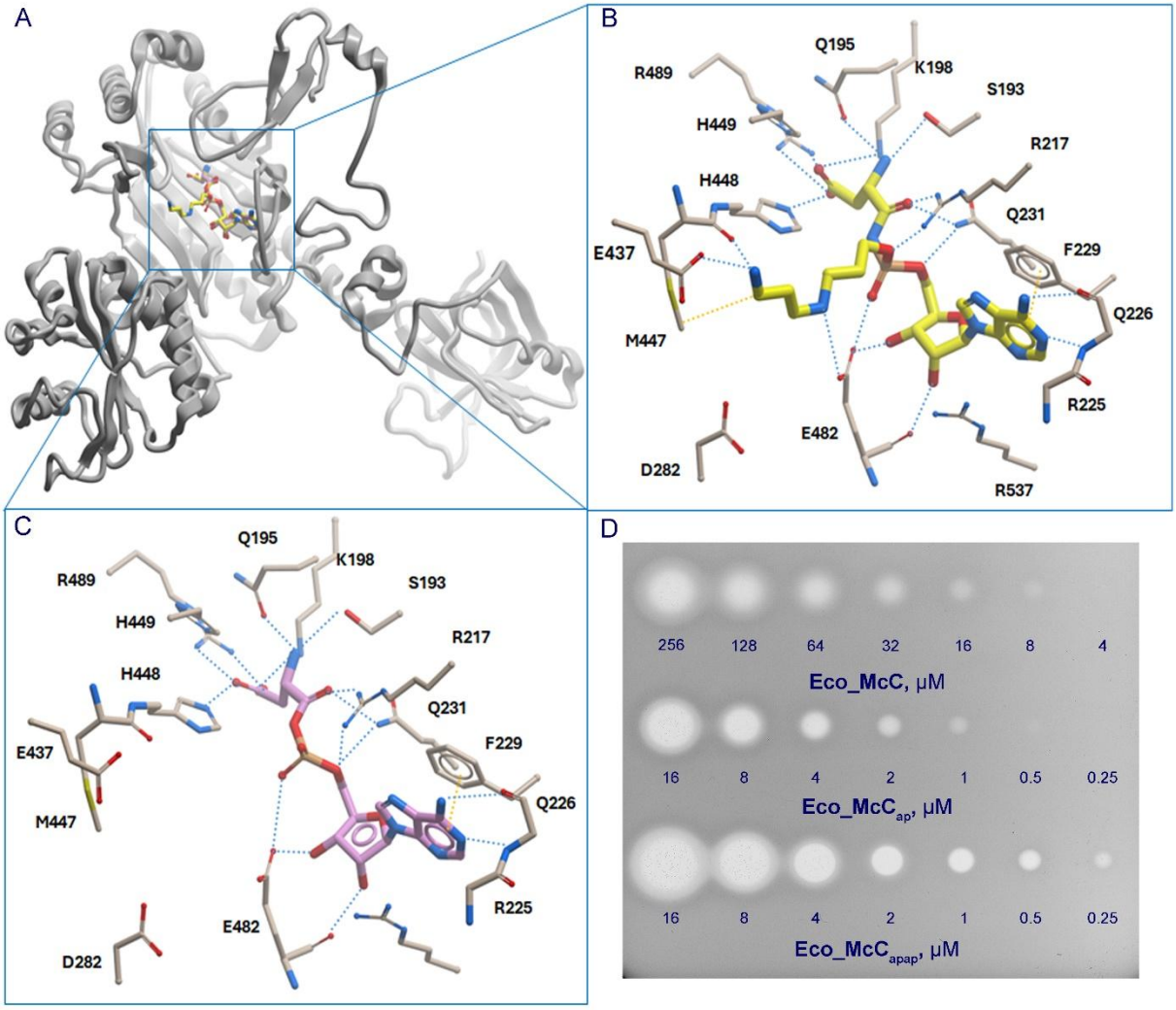

Figure 5. (A) Structure of *E. coli* AspRS/tRNA^{Asp} complex with the natural substrate aspartyl-adenylate (PDB: 1c0a) and with superimposed tandem-aminopropylated isoasparagine-adenylate docked into the enzyme active center using CB-Dock2 homologous template fitting server and further refined with the docking package of Molsoft ICM-Pro. The protein is shown in grey ribbons, and the aspartyl-adenylate/tandem-aminopropylated isoasparagine-adenylate are shown as thick CPK-colored sticks, except carbon atoms are in pink and yellow, respectively. The tRNA is removed for clarity. The insets (B) and (C) are the zoom-in views of the selected area in AspRS, showing the contacts of the respective ligands with the residues of the substrate-binding pocket (thin CPK-colored sticks, except carbon atoms are in beige) located at interacting distances of <3.5Å. Dashed lines indicate likely polar (blue) and hydrophobic (yellow) interactions. (D) Tandem aminopropylation increases the bioactivity of *E. coli* McC. Minimal inhibitory concentration (MIC) of *E. coli* McC antibiotics without secondary modification (*Eco*-McC), and with a single (*Eco*-McC$_{ap}$) and tandem aminopropyl groups (*Eco*-McC$_{apap}$). MIC of the compound is defined as a minimal concentration at which a growth inhibition zone is visible in a drop diffusion assay.

The model also suggests that the warhead placement in the catalytic pocket does not interfere with the tRNA binding. Instead, the phosphates of the tRNA 3'-terminal dinucleotide electrostatically attract the positively charged amines of *Bsu*-McC aminopropyl groups, further stabilizing its binding to AspRS (Figure S14A). Moreover, the presence of tRNA in the complex with AspRS sterically blocks access to the active site pocket, hindering the *Bsu*-McC warhead dissociation (Figure S14B). These observations suggest that the extended interactions of the two aminopropyl groups with AspRS and tRNA should enhance the stability of the enzyme-inhibitor complex. Therefore, similar to the warhead of the *Eco*-McC, the warhead of *Bsu*-McC is expected to inhibit the activity of *E. coli* aspartyl-tRNA synthetase.

Inspired by our *in-silico* model, we generated a doubly aminopropylated *E. coli* McC by using purified E. coli McC (*Eco*-McC_{ap}) as a substrate for aminopropylation by $MccM2^{Bsu}$ in the presence of dcSAM (Figure S15). The unmodified (*Eco*-McC), mono-aminopropylated (*Eco*-McC_{ap}), and tandem-aminopropylated (*Eco*-McC_{apap}) compounds were evaluated for their inhibitory activity towards McC-sensitive *E. coli* BL21 using drop-diffusion assay. Results showed that the 0.25 µM *Eco*-McC_{apap} produced a growth inhibition zone comparable to 1 µM mono-aminopropylated peptidyl-adenylate or 8 µM unmodified *E. coli* peptidyl-adenylate (Figure 5D). As expected, moderate overexpression of AspRS, but not ProRS, protected *E. coli* BL21 against *Eco*-McC_{ap} and *Eco*-McC_{apap} toxicity (Figure S16). These findings are in line with our *in-silico* prediction, revealing that the addition of the second aminopropyl group significantly enhances *Eco*-McC's toxicity against *E. coli* BL21, reducing the apparent MIC by 4-fold and 32-fold compared to the mono-aminopropylated and unmodified compounds, respectively.

Production of *Bsu*-McC changes the social behavior of *B. subtilis* strains.

While studying the *Bsu*-McC biosynthesis, we noticed that *B. subtilis* 168 harboring the plasmid expressing *mccCM1BAM2*^{Bsu} exhibited colony morphology different from that of the same strain carrying an empty vector as control. To take a closer look at the impact of *Bsu*-McC production on the social behavior of bacteria, we examined the ability of the biofilm-proficient *B. subtilis* 3A38 strain harboring plasmid expressing *mccCM1BAM2*^{Bsu} to form biofilms. As expected, *B. subtilis* 3A38, which carries the control vector, produces a compact wrinkled biofilm structure after one day of growth on modified LB agar (Figure 6A). In contrast, under the same growth conditions, *B. subtilis* 3A38 harboring plasmids expressing either minimal *mccCBA*^{Bsu} or complete *mccCM1BAM2*^{Bsu} BGC does not form biofilm. Instead, it forms a thin layer of actively

growing bacteria (Figure 6A). To confirm the *mcc*^{Bsu}-dependent change in colony morphology, we constructed a *B. subtilis* MG27 *mccB*^{Bsu}-null mutant (*mccB*^{Bsu}Ω*loxP*) strain and tested it for biofilm formation. As shown in Figure 6B, the wild-type *Bsu*-McC-producer strain forms a large diffuse actively growing macro-colony on the modified LB agar, distinct from that of biofilm-deficient Δ*speD* mutant. Under the same conditions, the isogenic *mccB*^{Bsu}-null mutant cells readily formed a well-developed, thick, wrinkled biofilm (Figure 6B).

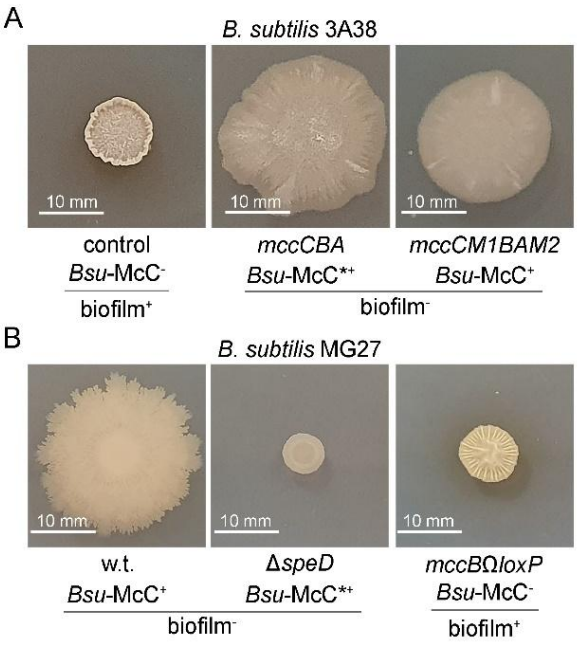

Figure 6. McC^{Bsu} production changes the social behavior of *B. subtilis*. (A) Expression of *mcc*^{Bsu} BGC prevents biofilm formation in heterologous hosts. *B. subtilis* 3A38 strain harboring either an empty pHT01 vector or pHT01 expressing indicated *mcc*^{Bsu} genes were grown on the biofilm-inducing modified LB agar supplemented with IPTG for 24 h. (B) Inactivation of *Bsu*-McC production renders the native producer *B. subtilis* MG27 strain biofilm-proficient. *B. subtilis* MG27 w.t., Δ*speD* mutant, and *mccB*^{Bsu} null mutant (*mccB*Ω*loxP*) were grown on modified LB agar for 24 h. *B. subtilis* MG27 Δ*speD* mutant was used as a biofilm-negative control. Strains used in the biofilm-formation tests produced either no *Bsu*-McC ("*Bsu*-McC^{-}"), adenylated peptide only ("*Bsu*-McC*$^{+}$"), or tandem–aminopropylated microcin C ("*Bsu*-McC^{+}").

The absence of a biofilm-producing phenotype may result either from an unknown signaling function of *Bsu*-McC or from a metabolic perturbation in the *Bsu*-McC-producer cells. To test if *Bsu*-McC can act as a paracrine signal molecule that alters cell differentiation and complex colony morphology, we repeated the biofilm formation experiment using the modified LB agar supplemented with *Bsu*-McC. However, no reversal of phenotype was detected under these condi-

tions (Figure S17). This observation indicates that the primary cause of the observed changes in colony morphology is the perturbation in cell metabolic state upon *Bsu*-McC production.

DISCUSSION

Secondary modifications such as macrocyclization, oxidation, hydroxylation, dehydration, epimerization, acylation, glycosylation, *etc*., are common in RiPPs.[29] These modifications are necessary for enhancing bioactivity,[30,31] improving stability of the molecules,[22,32] or overcoming resistance.[9] Among the enzymes involved in the secondary modification of natural compounds, SAM-dependent methyltransferases are among the most common. These enzymes typically use SAM as a methyl group donor, transferring it to a heteroatom or, less often, to a carbon atom in RiPPs.[33] In contrast, the use of SAM as an ACP donor is very rare, with only a few known biochemical reactions. These include posttranscriptional modification of tRNAs[34] and biosynthesis of siderophores such as staphylopine[35] and pseudopaline,[36] the antibiotic nocardicin A,[37] and several other small molecules.[38] Unlike most other natural compounds, the biosynthesis of McC relies on SAM as a source of the aminopropyl group. Consequently, decarboxylation of the ACP group should occur either before or after its transfer to the phosphate moiety of McC. In *E. coli* or *Y. pseudotuberculosis* McC, the aminopropylation reaction involves two steps: first, aminocarboxypropyltransferase MccD transfers the ACP group to the phosphate of the peptidyl-nucleotide compound, followed by ACP decarboxylation by pyridoxal-5′-phosphate (PLP)-dependent decarboxylase MccE1 (Figure 1B).[9,19] Interestingly, similar coupled reactions were described in the biosynthesis of several natural translocase I inhibitors, including caprazamycin, sphaerimicin, muraymycin, and others. However, the first step in these reactions is catalyzed by an unusual PLP-dependent aminobutyryltransferase, while the decarboxylation step is performed by Mur23,[39] which is homologous to MccE1 (22 % sequence identity).

The AlphaFold-predicted structures of *B. subtilis* 3-aminopropyltransferases, MccM1^{Bsu} and MccM2^{Bsu},[40] exhibit significant structural homology with the 3-amino-3-carboxyaminopropyltransferase MccD^{Eco} (Suppl Fig. S18). However, unlike MccD^{Eco}, they show high specificity for dcSAM as the aminopropyl group donor (Figure 5C, Figures S10 and S12). The structural determinants that restrict the substrate specificity of these enzymes to dcSAM remain to be elucidated. Notably, dcSAM is a key intermediate in the biosynthesis of spermidine

and spermine, which are found in both prokaryotic[41] and eukaryotic[42] cells. To the best of our knowledge, MccM1^{Bsu} and MccM2^{Bsu} are the first known enzymes outside the polyamine biosynthetic pathway to utilize dcSAM as a substrate.

Using dcSAM as an aminopropyl donor may seem like a more efficient strategy and, therefore, might be expected to be more widespread in nature. However, *mcc* BGCs containing the *mccD-mccE1* gene pair are found across diverse bacterial phyla,[17] while BGCs encoding *mccM1/mccM2* homologs are restricted to a small subset of Bacilli. This distribution may reflect the metabolic cost of producing aminopropylated McC within the cell. For instance, disruption of the spermidine biosynthetic pathway inhibits planktonic growth of Gram-negative bacteria,[43] whereas Gram-positive *B. subtilis*[44] and *Streptococcus pneumoniae*[45] can grow normally without producing spermidine. This suggests that repurposing a portion of the cellular dcSAM pool toward McC-ap biosynthesis may impose a smaller fitness burden on Gram-positive than Gram-negative bacteria. Additionally, unlike SAM, dcSAM is not a universal metabolite. Many bacteria lack SAM decarboxylase and instead rely on alternative spermidine biosynthesis pathways that bypass dcSAM.[46] Thus, using SAM as a source of 3-amino-3-carboxypropyl group, which requires further decarboxylation of the intermediate product by a dedicated enzyme like MccE1 represents a more adaptive aminopropylation strategy. This versatility may have contributed to the broader distribution of BGCs containing *mccD*/*mccE1* homologs across bacterial species.

Adding a single aminopropyl group to McC enhances its bioactivity eightfold, while the second aminopropyl group increases it fourfold further (Figure 5D). This dramatic increase likely results from improved molecular fit and stability within the AspRS active site, which leads to more effective enzyme inhibition. Our structural modeling supports this view, providing insights into the molecular basis for the improved inhibitory efficacy. The model suggests that extended interactions of the two aminopropyl groups with the AspRS active center residues, as well as with the phosphates of the tRNA 3'-terminal nucleotides, stabilize the enzyme-inhibitor complex and sterically hinder the *Bsu*-McC warhead dissociation. These findings highlight the potential of aminopropylated derivatives of McC as templates for designing potent AspRS inhibitors. Such inhibitors could serve as valuable tools in developing novel antimicrobial agents, especially against resistant bacterial strains. Further investigations of *Bsu*-McC biosynthesis and its structural properties may inspire innovative approaches for engineering RiPP-based antibiotics with enhanced specificity, greater efficacy, and reduced susceptibility to resistance mechanisms.

B subtilis are among the most prevalent microbes in the rhizosphere, competing with diverse bacterial species.[47] Production of antibiotics and quorum sensing inhibitors, as well as the formation of root-associated biofilms, are the bases for effective biocontrol and prevention of bacterial diseases of plants.[48–50] Although the effects of *Bsu*-McC on the soil microbiome remain unknown, we observed an unexpected impact on the social behavior of the producer strain. Both natural *Bsu*-McC producer *B. subtilis* MG27 and the laboratory strain of *B. subtilis* 3A38 heterologously expressing mcc^{Bsu} exhibited reduced biofilm formation (Figure 6). Unlike some RiPPs (e.g., lanthipeptides SapB,[51] AmfS,[3] and SapT[52]) that induce morphogenic effects like sporulation in certain *Streptomyces* strains, *Bsu*-McC inhibits rather than promotes biofilm formation and does not act as a paracrine signal on bacilli if supplemented in trans (Figure S17). Its production likely disrupts metabolic pathways, slowing down the complex regulatory cascade that leads to biofilm development.[53,54] For instance, *Bsu*-McC biosynthesis could cause a reduction of cellular dcSAM concentration, thus hindering spermidine synthesis and postponing bacilli entering the biofilm state.[44] However, deletion of $mccM1^{Bsu}/M2^{Bsu}$ did not rescue this phenotype (Figure 6), suggesting the effect is not due to reduced dcSAM or spermidine synthesis.[44]

A second possible explanation is ATP depletion in cells actively producing the peptidyl-adenylate. In *B. subtilis*, the expression of many genes strongly depends on the cytoplasmic levels of ATP or GTP.[55] Biosynthesis of *Bsu*-McC might elevate (p)ppGpp levels, as seen in *E. coli*, where AspRS activity is inhibited by accidentally released McC warhead, eliciting stringent response.[56] Accumulation of high levels of (p)ppGpp with concomitant depletion of the intracellular concentration of GTP may lock *B. subtilis* cells in a motile state, preventing their differentiation and biofilm formation.[57] This could explain the actively growing flat colony morphology observed in *Bsu*-McC-producing *B. subtilis* strains. Whether the *Bsu*-McC biosynthesis depletes the cellular energy pools or triggers complex regulatory cascades warrants further investigation, which could reveal novel insights into microbial physiology.

EXPERIMENTAL SECTION

Bacterial strains and growth conditions

B. subtilis MG27 strain was generously provided by Prof. Oscar P. Kuipers (University of Groningen, Groningen, the Netherlands). *B. subtilis* 168 and 3A38 strains (Bacillus Genetic Stock

Center, USA) were used as heterologous hosts for the *mcc*^{Bsu} production. Cloning was performed in *E. coli* NEB5α (NEB). *E. coli* BL21 (DE3) strain (NEB) was used as a protein expression host. *E. coli* BL21 strain (NEB) was used for the McC susceptibility tests. *E. coli* BW25113 Δ*yejA* from the KEIO collection[58] was used to purify *E. coli* McC lacking the aminopropylated group. *E. coli* and *B. subtilis* strains were routinely grown in LB supplemented with appropriate antibiotics and inductors as required.

Molecular cloning and strain construction

The genomic DNA of *B. subtilis* MG27 and the corresponding primers listed in Table S2 were used for PCR amplification of *mcc*^{Bsu} BGC and individual genes. To verify MccE2^{Bsu} immunity role, *mccE2*^{Bsu} was cloned into a pBAD_SalRBS vector[59] derived from pBAD-His (Invitrogen), between SalI and HindIII. *mccB*^{Bsu} was inserted into the pET22_MBP plasmid[60] between BamHI and XhoI to create an in-frame fusion with N-terminal MBP. For heterologous production of C-terminally his-tagged MccM1^{Bsu} and MccM2^{Bsu}, corresponding PCR-amplified genes were inserted between NdeI and XhoI of the same vector, replacing *mbp*. For heterologous expression of *mcc*^{Bsu} BGC variants in *B. subtilis*, *mccCM1BAM2*^{Bsu} and *mccCM1BA*^{Bsu} were inserted between BamHI and EagI of the modified pHT01 *E. coli-B. subtilis* shuttle vector (MoBiTech).[22] pHT-*mccCBAM2*^{Bsu} and pHT-*mccCBA*^{Bsu} vectors were constructed using overlap-extension PCR[61] of *mccC*^{Bsu} and *mccBAM2*^{Bsu} or *mccBA*^{Bsu}, respectively, and subsequent cloning as above.

B. subtilis 168 and MG27 mutants were constructed using a single cross-over pSC vector and Cre-*loxP* recombination system described in ref.[62]. *B. subtilis* MG27 *mccB*^{Bsu}Ω*loxP* was constructed by sequential integration and excision of the pSC vector containing a 300-bp *mccB*^{Bsu} fragment. *B. subtilis* MG27 and 168 Δ*speD* mutants were constructed using two rounds of insertion-excision of the pSC vector with the corresponding DNA fragments upstream and downstream of *speD*. The second excision of the integrated plasmid resulted in a single *loxP* site in the place of *speD*.

Protein extraction and purification

Vectors pCA24-*pepB*, pCA24-*pepN*, pCA24-*speD* purified from ASKA collection strains[63] were used for His-PepB, His-PepN, and His-SpeD^{Eco} production, respectively. For protein expression, 4 mL of an overnight culture of *E. coli* BL21(DE3) harboring corresponding vector were inoculated to 400 mL of LB medium containing either 100 µg/mL of ampicillin (for

pET22_MBP-*mccB*^{Bsu}, pET22_*mccM1*^{Bsu}, pET22_*mccM2*^{Bsu}) or 34 µg/mL of chloramphenicol (for pCA24-*pepB*, pCA24-*pepN*, pCA24-*speD*). Cultures were grown at 37 °C with vigorous shaking until the OD_{600} reached ~0.6. Then cell cultures were cooled down in iced water for 10 min, induced with 0.25 mM IPTG , and moved to grow at 18 °C for 20 H with moderate shaking. Cells were harvested by centrifugation at 3 500 x *g* at 4 °C for 20 min, resuspended in 20 mL of buffer containing 20 mM Tris-HCl pH 8.0, 500 mM NaCl, and 10% glycerol, and frozen at -80 °C. Upon thawing on ice, phenylmethylsulfonyl fluoride (PMSF) was added up to 1 mM, and then cells were lysed by sonication. Obtained lysates were clarified by centrifugation at 15 000 x *g* at 4 °C for 1 h.

For the MBP-MccB^{Bsu} purification, the cleared lysate was loaded on the MBPTrap HP 1 mL column (Cytiva) prewashed with TSG buffer (20 mM Tris-HCl pH 8.0, 150 mM NaCl, 10% glycerol). The column was washed with 20 mL of TSG buffer following the protein elution with TSG buffer supplemented with 10 mM maltose. For further purification, protein fractions were filter-concentrated using an Amicon Ultra-15 Centrifugal Filter Unit with 30 kDa cut-off (Merck Millipore) and loaded on a HiLoad 16/600 Superdex 200 pg (Cytiva) gel-filtration column equilibrated with 20 mM Tris-HCl pH 8.0, 150 mM NaCl buffer and eluted with 1 mL/min flow rate.

To purify MccM1^{Bsu}-His, MccM2^{Bsu}-His, His-SpeD, His-PepB, or His-PepN, the respective cleared lysates were loaded on the HiTrap TALON crude 1 mL column (Cytiva) prewashed with the TSG buffer. After the washing step with 20 mL of TSG buffer supplemented with 5 mM imidazole, the proteins were eluted by a linear 5 to 250 mM gradient of imidazole in the TSG buffer. For further purification, fractions containing the protein of interest were buffer-exchanged to 20 mM Tris-HCl pH 8.0, 50 mM NaCl, and 5% glycerol and then loaded on MonoQ column 5/50 GL (Cytiva). After washing with 20 mM Tris-HCl pH 8.0, 50 mM NaCl, the proteins were eluted in a 20-min linear gradient of NaCl (0.05 to 1 M) in 20 mM Tris-HCl pH 8.0 buffer with 1 mL/min flow rate. His-tagged 5'-methylthioadenosine/S-adenosylhomocysteine nucleosidase Mtn^{Eco} was purified as described in ref.[19]

The purity of recombinant proteins was >95%, as judged by Coomassie Brilliant Blue staining after SDS-PAGE. The concentration of proteins was determined by absorption at wavelength 280 nm using the theoretical extinction coefficient.

***B. subtilis* and *E. coli* McCs extraction and purification**

Vectors pA7 and pA7-ap[13] transformed to *E. coli* BW25113 Δ*yejA*[58] were used to produce *Eco*-McC peptide adenylate and *Eco*-McC_{ap} aminopropylated peptide adenylate, respectively. *Bsu*-McC was produced heterologously in *B. subtilis* 168 harboring pHT-*mccCM1BAM2*^{Bsu} vector.

The corresponding overnight cultures grown in 100 mL of LB supplemented with 100 µg/mL ampicillin (*E. coli*) or 10 µg/mL chloramphenicol (*B. subtilis*) at 37 °C were pelleted at 3 500 x *g* for 10 min. *Eco*-McC and *Eco*-McC_{ap}-producing *E. coli* strains were resuspended in 1 L of M9 minimal medium supplemented with 3 µg/mL thiamine, 0.02% yeast extract, 0.2% glycerol, 0.2% glucose, 0.02% casamino acids and 100 µg/mL ampicillin. The cells were grown at 37 °C with vigorous shaking for 18 h. *Bsu*-McC-producing *B. subtilis* 168 strain was resuspended in M9 minimal medium supplemented with 50 µg/mL L-tryptophan, 0.02% yeast extract, 0.4% sorbitol, trace elements (134 µM EDTA, 31 µM $FeCl_3$, 6.2 µM $ZnCl_2$, 0.76 µM $CuCl_2$, 0.42 µM $CoCl_2$, 1.62 µM H_3BO_3, 0.081 µM $MnCl_2$), 10 µg/mL chloramphenicol, and 0.1 mM IPTG. The culture was incubated at 37 °C with vigorous shaking for 2.5 days.

Cells were pelleted by centrifugation at 10 000 x *g* for 1 h. The supernatants were collected, filtered through the 0.45 µm membrane filter (Durapore, Merck Millipore), supplemented with TFA up to 0.3%, and loaded on the C18 cartridge (Mega Bond Elut C18 10 g, Agilent Technologies). The column was washed with 100 mL of 2.5% acetonitrile in 0.1% TFA and eluted with 15% acetonitrile in 0.1% TFA. The microcin-containing fractions were vacuum-dried. The pellets were dissolved in 0.1% TFA and loaded on the Zorbax Eclipse Plus C18 column (5 µm, 4.6 x 250 mm, Agilent Technologies) for reverse-phase HPLC purification. McCs were eluted in a 30-min 0 to 15% linear acetonitrile gradient in 0.1% TFA with 1 mL/min flow rate and absorption detection at 260 nm and 280 nm. Fractions containing McCs were verified by mass spectrometry, dried, and stored at -20°C.

The published extinction coefficient for adenosine monophosphate (E^{mM} = 15.4 at 259 nm at pH 7.0) was used to calculate peptidyl-nucleotide concentrations.[64]

Processing of peptide part of *Bsu*-McC and NMR analysis

To process the peptide part of *Bsu*-McC 100 µM of the compound was incubated at 30 °C with 10 µM PepB and 5 µM PepN aminopeptidases and 1 mM $MnCl_2$ in 20 mM HEPES-NaOH buffer, pH 7.5, for 16 h. The reaction was quenched with an equal volume of 0.1% TFA in acetonitrile. The mixture was incubated 30 min at 4 °C before centrifugation at 20 000 x *g* at 4 °C for

15 min. The supernatant was vacuum-dried, resuspended in 0.1% TFA, and loaded on Prep-C18 (100Å, 5 µm, 10 x 250 mm, Agilent Technologies) HPLC column. Processed *Bsu*-McC was eluted in a 30-min 0% to 20% gradient of acetonitrile in 0.1% TFA at 3 mL/min flow rate.

NMR spectra were acquired at 293 K on an 800 MHz Bruker Neo spectrometer (Bruker Biospin, Billerica, USA), equipped with a QCPN cryoprobe. The initial sample contained 3.4 mg of partially processed *Bsu*-McC dissolved in 200 µl of a 90%/10% H_2O/D_2O solution at pH ~5. TOCSY and ROESY spectra were acquired as matrices of 16k x 512 points, sampling a window of 12ppm centered at 4.70 ppm in both dimensions, with 4 respectively 32 scans per increment. The ^{1}H, ^{15}N HSQC spectrum was acquired as a matrix of 2k x 128 complex points, sampling a window of 12 ppm centered at 4.70 ppm in the ^{1}H dimension and of 36 ppm centered at 119 ppm in the ^{15}N dimension, with 128 scans per increment. The ^{1}H, ^{13}C HSQC and dipsi-HSQC spectra were recorded as matrices of 2k x 256 points, sampling a window of 12 ppm centered at 4.70 ppm in the ^{1}H dimension and of 80 ppm centered at 40 ppm in the ^{13}C dimension, with 32 and 64 scans per increment, respectively. J resolved experiments with or without ^{31}P π pulse in the t_1 evolution period were recorded with 16k x 64 points covering spectral windows of 12 ppm and 60 Hz in the direct and indirect dimensions. All spectra were processed with Topspin4.1 (Bruker Biospin, Billerica).

Reconstitution of *Bsu*-McC biosynthesis *in vitro*

To obtain dcSAM, 0.5 mM SAM was incubated with 5 µM recombinant $SpeD^{Eco}$ in 50 mM HEPES-NaOH pH 7.5 buffer supplemented with 50 mM NaCl at 30 °C for 16h. The reaction was stopped by the addition of an equal volume of 0.2% TFA in acetonitrile, incubated for 30 min on ice, and centrifuged at 20 000 x *g* for 15 min at 4 °C. The supernatant was collected and lyophilized. The pellet was then resuspended in 7.5% methanol in 15 mM ammonium acetate buffer, pH 3.5, and loaded on YMC-Triart C18 (S-5µm, 150 x 4.6 mm, YMC Europe) column for the isocratic elution at 1 mL/min flow rate.

For in vitro adenylation, 50 µM of chemically synthesized MccABsu peptide (Genescript) was incubated with 3 µM of recombinant MBP-MccBBsu in 50 mM Tris-HCl pH 8.0 buffer supplemented with 10 mM MgCl2, 2 mM ATP, 5 mM DTT, and 150 mM NaCl at 28 °C for 16 h. The reaction was stopped by adding an equal volume of 0.2% TFA in acetonitrile, incubated for 30 min on ice, and centrifuged at 20 000 x g for 15 min at 4 °C. The supernatant was vacuum dried. The pellet was resuspended in 0.1% TFA and loaded on YMC-Triart C18 (S-5µm, 150 x 4.6 mm,

YMC Europe) for reverse-phase HPLC. The peptide-adenylate was eluted in a 20-min 0% to 50% gradient of acetonitrile in 0.1% TFA at 1 mL/min flow rate.

To reconstitute the di-aminopropylation pathway in vitro, 250 μM dcSAM and 50 μM adenylated MccABsu were combined with 5 μM MccM1Bsu or 5 μM MccM2Bsu, or both, in the presence of 1.5 μM MtnEco, 250 μM tris(2-carboxyethyl)phosphine (TCEP), and 50 mM HEPES pH 7.5. Reactions were incubated at 30 °C for 16 h. For MS analysis, reactions were then quenched by adding TFA up to 0.1%, and desalted using C18 ZipTip Pipette Tips (Millipore). To purify the aminopropylated products from corresponding in vitro reactions the same protocol was used as for MccBBsu reaction purification.

In vitro synthesis and purification of di-aminopropylated McC^{Eco}

100 μM *Eco*-McC$_{ap}$ was incubated with 5 μM MccM2^{Bsu} in the presence of 0.5 mM SAM, 3 μM SpeD^{Eco}, 0.5 mM TCEP, and 1.5 μM Mtn^{Eco} in 3 mL of 50 mM HEPES-NaOH pH 7.5 buffer. The reaction was incubated at 30 °C for 24 h and then quenched with an equal volume of 0.2 % TFA in acetonitrile. After 30 min incubation at room temperature, the proteins were precipitated by centrifugation at 15 000 x *g* at 4 °C for 15 min. The supernatant was collected and vacuum-dried. The dried sample was dissolved in 0.1% TFA water solution, centrifuged at 15 000 x *g* for 15 min, and loaded on Prep-C18 (100Å, 5 μm, 10 x 250 mm, Agilent Technologies) column for HPLC purification. The di-aminopropylated form of *Eco*-McC (*Eco*-McC$_{apap}$) was separated at a 3 mL/min flow rate in a two-step gradient of acetonitrile in 0.1% TFA: 0 to 10% in 5 min, 10 to 12% in 10 min. The presence of *Eco*-McC$_{apap}$ in the collected fractions was verified by MS analysis. The corresponding fractions were vacuum dried, resuspended in 0.1% TFA, and subjected to a second round of reverse-phase HPLC on Triart C18 (S-5 μm, 150 x 4.6 mm, YMC Europe) column. *Eco*-McC$_{apap}$ was eluted in a 10-min 0% to 20% gradient of acetonitrile in 0.1% TFA at 1 mL/min flow rate. The purified compound was vacuum dried and stored at -20 °C.

Mass spectrometric analysis

For MALDI-TOF analysis, liquid samples or cells harvested from agar plates were mixed in 2:1 ratio with the matrix solution (20 mg/mL 2,5-dihydroxybenzoic acid (Sigma), 0.5% trifluoroacetic acid (TFA) in 30 % acetonitrile) on a steel target plate. Reflector mode on the UltrafleXtreme II MALDI-TOF-TOF (Bruker Daltonics), equipped with a neodymium laser

(355 nm), was used to detect mass/charge ratio (*m/z*) values of molecular ions with measurement accuracy within 0.1 Da. LIFT mode was used to obtain fragmentation spectra with the accuracy for the product ions within the 1 Da range. Mass-spectra processing was performed via FlexAnalysis 3.2 software (Bruker).

The high-resolution mass spectrometry analysis was performed as a part of LC-MS analysis on Agilent 1200 HPLC equipped with the UV and 6550 iFunnel QTOF LC/MS detectors and Jet Stream Technology ion source (Agilent Technologies). The analyzed compounds were loaded on Poroshell 120 SB-C18 column (2.7 µ, 2.1 x 100 mm, Agilent Technologies) at 40 °C using a linear (0 to 80%) gradient of acetonitrile in 5 mM ammonium acetate buffer (pH 5.2) at 0.2 mL/min flow rate. The electrospray source was set to positive ion mode at 4 kV, 290 °C. Data were analyzed using MassHunter Qualitative Analysis 10.00 software (Agilent Technologies).

Morphological assays

The cultures of tested strains were grown in 5 mL LB media at 37 °C with vigorous shaking for 20 hours. 2-µL drops of the cultures were placed on the surface of the modified LB agar (1% Tryptone, 0.5% yeast extract, 0.5% NaCl, 2% glycerol, 20 µM $MnCl_2$.and 2.5% agar) for biofilm development.[65] Plates were incubated at 37 °C for 24 hours.

McC susceptibility drop diffusion assay

100-µL aliquot of an overnight culture of *E. coli* BL21 cells carrying either empty pBAD_SalRBS plasmid, pBAD-*mccE2*^{Bsu} , pBAD-*aspS* or pBAD-*proS* were inoculated into 20 mL of warm LB medium containing 1% agar and 100 µg/ml ampicillin poured into a Petri dish and allowed to solidify. For *mccE2*^{Bsu} immunity test and *aspS*/*proS* protection test, the soft agar was additionally supplemented with 1- and 10-mM arabinose, respectively. 3-µl drops of the serially diluted McC solutions were deposited on the surface of the soft agar and allowed to absorb. Plates were incubated at 37 °C for 12 h to form bacterial lawn, and the growth inhibition zones became visible. The compound's minimal inhibitory concentration (MIC) was defined as a minimal concentration of an antibiotic at which the growth inhibition zone was observable.

ASSOCIATED CONTENT

MALDI TOF and MALDI TOF/TOF spectra, NMR spectra, HPLC chromatograms, bioactivity tests (Figures S1-S16) , as well as chemical shifts for *Bsu*-McC (Table S1) and list of primers used in the study (Table S2).

Funding Sources

This work was supported by a NIH R35 GM151874 to S.K.N., and RSF 21-74-00137 to A.K., intramural funds from Rowan University School of Osteopathic Medicine at Stratford, NJ, USA to S.B., fellowship of the Collège de France and the INRAe to S.D., and the RIKEN Junior Research Associate Program to A.P.

Notes

The authors declare no competing financial interest.

ACKNOWLEDGMENT

We are grateful to Prof. Oskar P. Kuipers (University of Groningen, Netherlands) for providing the native *Bsu*-McC producer and for the helpful discussion. We thank Dr. Shunsuke Tagami (RIKEN, Japan) for the fruitful discussion and valuable insights. We thank MetaboHub-MetaToul (Metabolomics and Fluxomics facilities, Toulouse, France (http://www.mth-metatoul.fr), part of the French National Infrastructure for Metabolomics and Fluxomics (http://www.metabohub.fr) funded by a grant from the Agence Nationale de la Recherche Scientifique (MetaboHUB-ANR-11-INBS-0010) for access to the NMR facility and the Moscow State University Development Programme APG 5.13 for access to the mass spectrometry facility.

REFERENCES

(1) Montalbán-López, M.; Scott, T. A.; Ramesh, S.; Rahman, I. R.; van Heel, A. J.; Viel, J. H.; Bandarian, V.; Dittmann, E.; Genilloud, O.; Goto, Y.; Grande Burgos, M. J.; Hill, C.; Kim, S.; Koehnke, J.; Latham, J. A.; Link, A. J.; Martínez, B.; Nair, S. K.; Nicolet, Y.; Rebuffat, S.; Sahl, H.-G.; Sareen, D.; Schmidt, E. W.; Schmitt, L.; Severinov, K.; Süssmuth, R. D.; Truman, A. W.; Wang, H.; Weng, J.-K.; van Wezel, G. P.; Zhang, Q.; Zhong, J.; Piel, J.; Mitchell, D. A.; Kuipers, O. P.; van der Donk, W. A. New Developments in RiPP Discovery, Enzymology and Engineering. *Nat Prod Rep* **2021**, *38* (1), 130–239. https://doi.org/10.1039/D0NP00027B.

(2) Nakayama, J.; Cao, Y.; Horii, T.; Sakuda, S.; Akkermans, A. D.; de Vos, W. M.; Nagasawa, H. Gelatinase Biosynthesis-Activating Pheromone: A Peptide Lactone That Mediates a Quorum Sensing in Enterococcus Faecalis. *Mol Microbiol* **2001**, *41* (1), 145–154. https://doi.org/10.1046/j.1365-2958.2001.02486.x.

(3) Ueda, K.; Oinuma, K.-I.; Ikeda, G.; Hosono, K.; Ohnishi, Y.; Horinouchi, S.; Beppu, T. AmfS, an Extracellular Peptidic Morphogen in Streptomyces Griseus. *J Bacteriol* **2002**, *184* (5), 1488–1492. https://doi.org/10.1128/JB.184.5.1488-1492.2002.

(4) Kenney, G. E.; Rosenzweig, A. C. Chemistry and Biology of the Copper Chelator Methanobactin. *ACS Chem Biol* **2012**, *7* (2), 260–268. https://doi.org/10.1021/cb2003913.

(5) Peña-Ortiz, L.; Graça, A. P.; Guo, H.; Braga, D.; Köllner, T. G.; Regestein, L.; Beemelmanns, C.; Lackner, G. Structure Elucidation of the Redox Cofactor Mycofactocin Reveals Oligo-Glycosylation by MftF. *Chem Sci* **2020**, *11* (20), 5182–5190. https://doi.org/10.1039/d0sc01172j.

(6) Hudson, G. A.; Mitchell, D. A. RiPP Antibiotics: Biosynthesis and Engineering Potential. *Curr Opin Microbiol* **2018**, *45*, 61–69. https://doi.org/10.1016/j.mib.2018.02.010.

(7) Arnison, P. G.; Bibb, M. J.; Bierbaum, G.; Bowers, A. A.; Bugni, T. S.; Bulaj, G.; Camarero, J. A.; Campopiano, D. J.; Challis, G. L.; Clardy, J.; Cotter, P. D.; Craik, D. J.; Dawson, M.; Dittmann, E.; Donadio, S.; Dorrestein, P. C.; Entian, K.-D. D.; Fischbach, M. A.; Garavelli, J. S.; Göransson, U.; Gruber, C. W.; Haft, D. H.; Hemscheidt, T. K.; Hertweck, C.; Hill, C.; Horswill, A. R.; Jaspars, M.; Kelly, W. L.; Klinman, J. P.; Kuipers, O. P.; Link, A. J.; Liu, W.; Marahiel, M. A.; Mitchell, D. A.; Moll, G. N.; Moore, B. S.; Müller, R.; Nair, S. K.; Nes, I. F.; Norris, G. E.; Olivera, B. M.; Onaka, H.; Patchett, M. L.; Piel, J.; Reaney, M. J. T.; Rebuffat, S.; Ross, R. P.; Sahl, H.-G. G.; Schmidt, E. W.; Selsted, M. E.; Severinov, K.; Shen, B.; Sivonen, K.; Smith, L.; Stein, T.; Süssmuth, R. D.; Tagg, J. R.; Tang, G.-L. L.; Truman, A. W.; Vederas, J. C.; Walsh, C. T.; Walton, J. D.; Wenzel, S. C.; Willey, J. M.; van der Donk, W. A. Ribosomally Synthesized and Post-Translationally Modified Peptide Natural Products: Overview and Recommendations for a Universal Nomenclature. *Nat Prod Rep* **2013**, *30* (1), 108–160. https://doi.org/10.1039/c2np20085f.

(8) Garcia-Bustos, J. F.; Pezzi, N.; Mendez, E. Structure and Mode of Action of Microcin 7, an Antibacterial Peptide Produced by Escherichia Coli. *Antimicrob Agents Chemother* **1985**, *27* (5), 791–797. https://doi.org/10.1128/aac.27.5.791.

(9) Tsibulskaya, D.; Mokina, O.; Kulikovsky, A.; Piskunova, J.; Severinov, K.; Serebryakova, M.; Dubiley, S. The Product of *Yersinia Pseudotuberculosis Mcc* Operon Is a Peptide-Cytidine Antibiotic Activated Inside Producing Cells by the TldD/E Protease. *J Am Chem Soc* **2017**, *139* (45), 16178–16187. https://doi.org/10.1021/jacs.7b07118.

(10) Novikova, M.; Metlitskaya, A.; Datsenko, K.; Kazakov, T.; Kazakov, A.; Wanner, B.; Severinov, K. The Escherichia Coli Yej Transporter Is Required for the Uptake of Translation Inhibitor Microcin C. *J Bacteriol* **2007**, *189* (22), 8361–8365. https://doi.org/10.1128/JB.01028-07.

(11) Kazakov, T.; Vondenhoff, G. H.; Datsenko, K. A.; Novikova, M.; Metlitskaya, A.; Wanner, B. L.; Severinov, K. Escherichia Coli Peptidase A, B, or N Can Process Translation Inhibitor Microcin C. *J Bacteriol* **2008**, *190* (7), 2607–2610. https://doi.org/10.1128/JB.01956-07.

(12) Metlitskaya, A.; Kazakov, T.; Kommer, A.; Pavlova, O.; Praetorius-Ibba, M.; Ibba, M.; Krasheninnikov, I.; Kolb, V.; Khmel, I.; Severinov, K. Aspartyl-TRNA Synthetase Is the Target of Peptide Nucleotide Antibiotic Microcin C. *J Biol Chem* **2006**, *281* (26), 18033–18042. https://doi.org/10.1074/jbc.M513174200.

(13) Zukher, I.; Pavlov, M.; Tsibulskaya, D.; Kulikovsky, A.; Zyubko, T.; Bikmetov, D.; Serebryakova, M.; Nair, S. K.; Ehrenberg, M.; Dubiley, S.; Severinov, K. Reiterative Synthesis by the Ribosome and Recognition of the N-Terminal Formyl Group by Biosynthetic Machinery Contribute to Evolutionary Conservation of the Length of Antibiotic Microcin C Peptide Precursor. *mBio* **2019**, *10* (2). https://doi.org/10.1128/mBio.00768-19.

(14) Roush, R. F.; Nolan, E. M.; Löhr, F.; Walsh, C. T. Maturation of an Escherichia Coli Ribosomal Peptide Antibiotic by ATP-Consuming N-P Bond Formation in Microcin C7. *J Am Chem Soc* **2008**, *130* (11), 3603–3609. https://doi.org/10.1021/ja7101949.

(15) Dong, S.-H.; Kulikovsky, A.; Zukher, I.; Estrada, P.; Dubiley, S.; Severinov, K.; Nair, S. K. Biosynthesis of the RiPP Trojan Horse Nucleotide Antibiotic Microcin C Is Directed by the N-Formyl of the Peptide Precursor. *Chem Sci* **2019**, *10* (8), 2391–2395. https://doi.org/10.1039/c8sc03173h.

(16) Serebryakova, M.; Tsibulskaya, D.; Mokina, O.; Kulikovsky, A.; Nautiyal, M.; Van Aerschot, A.; Severinov, K.; Dubiley, S. A Trojan-Horse Peptide-Carboxymethyl-Cytidine Antibiotic from Bacillus Amyloliquefaciens. *J Am Chem Soc* **2016**, *138* (48), 15690–15698. https://doi.org/10.1021/jacs.6b09853.

(17) Travin, D. Y.; Severinov, K.; Dubiley, S. Natural Trojan Horse Inhibitors of Aminoacyl-TRNA Synthetases. *RSC Chem Biol* **2021**, *2* (2), 468–485. https://doi.org/10.1039/d0cb00208a.

(18) Guijarro, J. I.; González-Pastor, J. E.; Baleux, F.; San Millán, J. L.; Castilla, M. A.; Rico, M.; Moreno, F.; Delepierre, M. Chemical Structure and Translation Inhibition Studies of the Antibiotic Microcin C7. *J Biol Chem* **1995**, *270* (40), 23520–23532. https://doi.org/10.1074/jbc.270.40.23520.

(19) Kulikovsky, A.; Serebryakova, M.; Bantysh, O.; Metlitskaya, A.; Borukhov, S.; Severinov, K.; Dubiley, S. The Molecular Mechanism of Aminopropylation of Peptide-Nucleotide Antibiotic Microcin C. *J Am Chem Soc* **2014**, *136* (31), 11168–11175. https://doi.org/10.1021/ja505982c.

(20) Li, Z.; Song, C.; Yi, Y.; Kuipers, O. P. Characterization of Plant Growth-Promoting Rhizobacteria from Perennial Ryegrass and Genome Mining of Novel Antimicrobial Gene Clusters. *BMC Genomics* **2020**, *21* (1), 157. https://doi.org/10.1186/s12864-020-6563-7.

(21) Novikova, M.; Kazakov, T.; Vondenhoff, G. H.; Semenova, E.; Rozenski, J.; Metlytskaya, A.; Zukher, I.; Tikhonov, A.; Van Aerschot, A.; Severinov, K. MccE Provides Resistance to Protein Synthesis Inhibitor Microcin C by Acetylating the Processed Form of the Antibiotic. *J Biol Chem* **2010**, *285* (17), 12662–12669. https://doi.org/10.1074/jbc.M109.080192.

(22) Grigoreva, A.; Andreeva, J.; Bikmetov, D.; Rusanova, A.; Serebryakova, M.; Garcia, A. H.; Slonova, D.; Nair, S. K.; Lippens, G.; Severinov, K.; Dubiley, S. Identification and Characterization of Andalusicin: N-Terminally Dimethylated Class III Lantibiotic from Bacillus Thuringiensis Sv. Andalousiensis. *iScience* **2021**, *24* (5), 102480. https://doi.org/10.1016/j.isci.2021.102480.

(23) Cox, N.; Millard, P.; Charlier, C.; Lippens, G. Improved NMR Detection of Phospho-Metabolites in a Complex Mixture. *Anal Chem* **2021**, *93* (11), 4818–4824. https://doi.org/10.1021/acs.analchem.0c04056.

(24) Wishart, D. S.; Guo, A.; Oler, E.; Wang, F.; Anjum, A.; Peters, H.; Dizon, R.; Sayeeda, Z.; Tian, S.; Lee, B. L.; Berjanskii, M.; Mah, R.; Yamamoto, M.; Jovel, J.; Torres-Calzada, C.; Hiebert-Giesbrecht, M.; Lui, V. W.; Varshavi, D.; Varshavi, D.; Allen, D.; Arndt, D.; Khetarpal, N.; Sivakumaran, A.; Harford, K.; Sanford, S.; Yee, K.; Cao, X.; Budinski, Z.; Liigand, J.; Zhang, L.; Zheng, J.; Mandal, R.; Karu, N.; Dambrova, M.; Schiöth, H. B.; Greiner, R.; Gautam, V. HMDB 5.0: The Human Metabolome Database for 2022. *Nucleic Acids Res* **2022**, *50* (D1), D622–D631. https://doi.org/10.1093/nar/gkab1062.

(25) Sekowska, A.; Coppée, J. Y.; Le Caer, J. P.; Martin-Verstraete, I.; Danchin, A. S-Adenosylmethionine Decarboxylase of Bacillus Subtilis Is Closely Related to Archaebacterial Counterparts. *Mol Microbiol* **2000**, *36* (5), 1135–1147. https://doi.org/10.1046/j.1365-2958.2000.01930.x.

(26) Yagmurov, E.; Gilep, K.; Serebryakova, M.; Wolf, Y. I.; Dubiley, S.; Severinov, K. S51 Family Peptidases Provide Resistance to Peptidyl-Nucleotide Antibiotic McC. *mBio* **2022**, *13* (3), e0080522. https://doi.org/10.1128/mbio.00805-22.

(27) Eiler, S.; Dock-Bregeon, A.-C.; Moulinier, L.; Thierry, J.-C.; Moras, D. Synthesis of Aspartyl-TRNAAsp in Escherichia Coli—a Snapshot of the Second Step. *EMBO J* **1999**, *18* (22), 6532–6541. https://doi.org/10.1093/emboj/18.22.6532.

(28) Liu, Y.; Yang, X.; Gan, J.; Chen, S.; Xiao, Z.-X.; Cao, Y. CB-Dock2: Improved Protein–Ligand Blind Docking by Integrating Cavity Detection, Docking and Homologous Template Fitting. *Nucleic Acids Res* **2022**, *50* (W1), W159–W164. https://doi.org/10.1093/nar/gkac394.

(29) Funk, M. A.; van der Donk, W. A. Ribosomal Natural Products, Tailored To Fit. *Acc Chem Res* **2017**, *50* (7), 1577–1586. https://doi.org/10.1021/acs.accounts.7b00175.

(30) Tocchetti, A.; Maffioli, S.; Iorio, M.; Alt, S.; Mazzei, E.; Brunati, C.; Sosio, M.; Donadio, S. Capturing Linear Intermediates and C-Terminal Variants during Maturation of the Thiopeptide GE2270. *Chem Biol* **2013**, *20* (8), 1067–1077. https://doi.org/10.1016/j.chembiol.2013.07.005.

(31) Cruz, J. C. S.; Iorio, M.; Monciardini, P.; Simone, M.; Brunati, C.; Gaspari, E.; Maffioli, S. I.; Wellington, E.; Sosio, M.; Donadio, S. Brominated Variant of the Lantibiotic NAI-107 with Enhanced Antibacterial Potency. *J Nat Prod* **2015**, *78* (11), 2642–2647. https://doi.org/10.1021/acs.jnatprod.5b00576.

(32) Velásquez, J. E.; Zhang, X.; van der Donk, W. A. Biosynthesis of the Antimicrobial Peptide Epilancin 15X and Its N-Terminal Lactate. *Chem Biol* **2011**, *18* (7), 857–867. https://doi.org/10.1016/j.chembiol.2011.05.007.

(33) Schröder, M.-P.; Pfeiffer, I. P.-M.; Mordhorst, S. Methyltransferases from RiPP Pathways: Shaping the Landscape of Natural Product Chemistry. *Beilstein journal of organic chemistry* **2024**, *20*, 1652–1670. https://doi.org/10.3762/bjoc.20.147.

(34) Meyer, B.; Immer, C.; Kaiser, S.; Sharma, S.; Yang, J.; Watzinger, P.; Weiß, L.; Kotter, A.; Helm, M.; Seitz, H.-M.; Kötter, P.; Kellner, S.; Entian, K.-D.; Wöhnert, J. Identification of the 3-Amino-3-Carboxypropyl (Acp) Transferase Enzyme Responsible for Acp3U Formation at Position 47 in Escherichia Coli TRNAs. *Nucleic Acids Res* **2020**, *48* (3), 1435–1450. https://doi.org/10.1093/nar/gkz1191.

(35) Ghssein, G.; Brutesco, C.; Ouerdane, L.; Fojcik, C.; Izaute, A.; Wang, S.; Hajjar, C.; Lobinski, R.; Lemaire, D.; Richaud, P.; Voulhoux, R.; Espaillat, A.; Cava, F.; Pignol, D.; Borezée-Durant, E.; Arnoux, P. Biosynthesis of a Broad-Spectrum Nicotianamine-like Metallophore in Staphylococcus Aureus. *Science* **2016**, *352* (6289), 1105–1109. https://doi.org/10.1126/science.aaf1018.

(36) McFarlane, J. S.; Lamb, A. L. Biosynthesis of an Opine Metallophore by Pseudomonas Aeruginosa. *Biochemistry* **2017**, *56* (45), 5967–5971. https://doi.org/10.1021/acs.biochem.7b00804.

(37) Reeve, A. M.; Breazeale, S. D.; Townsend, C. A. Purification, Characterization, and Cloning of an S-Adenosylmethionine-Dependent 3-Amino-3-Carboxypropyltransferase in Nocardicin Biosynthesis. *J Biol Chem* **1998**, *273* (46), 30695–30703. https://doi.org/10.1074/jbc.273.46.30695.

(38) Lee, Y.-H.; Ren, D.; Jeon, B.; Liu, H.-W. S-Adenosylmethionine: More than Just a Methyl Donor. *Nat Prod Rep* **2023**, *40* (9), 1521–1549. https://doi.org/10.1039/d2np00086e.

(39) Cui, Z.; Overbay, J.; Wang, X.; Liu, X.; Zhang, Y.; Bhardwaj, M.; Lemke, A.; Wiegmann, D.; Niro, G.; Thorson, J. S.; Ducho, C.; Van Lanen, S. G. Pyridoxal-5'-Phosphate-Dependent Alkyl Transfer in Nucleoside Antibiotic Biosynthesis. *Nat Chem Biol* **2020**, *16* (8), 904–911. https://doi.org/10.1038/s41589-020-0548-3.

(40) Yang, Z.; Zeng, X.; Zhao, Y.; Chen, R. AlphaFold2 and Its Applications in the Fields of Biology and Medicine. *Signal Transduct Target Ther* **2023**, *8* (1), 115. https://doi.org/10.1038/s41392-023-01381-z.

(41) Michael, A. J. Polyamine Function in Archaea and Bacteria. *J Biol Chem* **2018**, *293* (48), 18693–18701. https://doi.org/10.1074/jbc.TM118.005670.

(42) Schibalski, R. S.; Shulha, A. S.; Tsao, B. P.; Palygin, O.; Ilatovskaya, D. V. The Role of Polyamine Metabolism in Cellular Function and Physiology. *Am J Physiol Cell Physiol* **2024**, *327* (2), C341–C356. https://doi.org/10.1152/ajpcell.00074.2024.

(43) Xie, Q. W.; Tabor, C. W.; Tabor, H. Deletion Mutations in the SpeED Operon: Spermidine Is Not Essential for the Growth of Escherichia Coli. *Gene* **1993**, *126* (1), 115–117. https://doi.org/10.1016/0378-1119(93)90598-w.

(44) Hobley, L.; Li, B.; Wood, J. L.; Kim, S. H.; Naidoo, J.; Ferreira, A. S.; Khomutov, M.; Khomutov, A.; Stanley-Wall, N. R.; Michael, A. J. Spermidine Promotes Bacillus Subtilis Biofilm Formation by Activating Expression of the Matrix Regulator SlrR. *J Biol Chem* **2017**, *292* (29), 12041–12053. https://doi.org/10.1074/jbc.M117.789644.

(45) Potter, A. J.; Paton, J. C. Spermidine Biosynthesis and Transport Modulate Pneumococcal Autolysis. *J Bacteriol* **2014**, *196* (20), 3556–3561. https://doi.org/10.1128/JB.01981-14.

(46) Hanfrey, C. C.; Pearson, B. M.; Hazeldine, S.; Lee, J.; Gaskin, D. J.; Woster, P. M.; Phillips, M. A.; Michael, A. J. Alternative Spermidine Biosynthetic Route Is Critical for Growth of Campylobacter Jejuni and Is the Dominant Polyamine Pathway in Human Gut Microbiota. *J Biol Chem* **2011**, *286* (50), 43301–43312. https://doi.org/10.1074/jbc.M111.307835.

(47) Vlamakis, H.; Chai, Y.; Beauregard, P.; Losick, R.; Kolter, R. Sticking Together: Building a Biofilm the Bacillus Subtilis Way. *Nat Rev Microbiol* **2013**, *11* (3), 157–168. https://doi.org/10.1038/nrmicro2960.

(48) Blake, C.; Christensen, M. N.; Kovács, Á. T. Molecular Aspects of Plant Growth Promotion and Protection by Bacillus Subtilis. *Mol Plant Microbe Interact* **2021**, *34* (1), 15–25. https://doi.org/10.1094/MPMI-08-20-0225-CR.

(49) Shi, W.-P.; Zeng, H.; Wan, C.-X.; Zhou, Z.-B. Amicoumacins from a Desert Bacterium: Quorum Sensing Inhibitor against Chromobacterium Violaceum. *Nat Prod Res* **2021**, *35* (23), 5508–5512. https://doi.org/10.1080/14786419.2020.1788554.

(50) Leistikow, K. R.; May, D. S.; Suh, W. S.; Vargas Asensio, G.; Schaenzer, A. J.; Currie, C. R.; Hristova, K. R. Bacillus Subtilis-Derived Peptides Disrupt Quorum Sensing and Biofilm Assembly in Multidrug-Resistant Staphylococcus Aureus. *mSystems* **2024**, e0071224. https://doi.org/10.1128/msystems.00712-24.

(51) Kodani, S.; Hudson, M. E.; Durrant, M. C.; Buttner, M. J.; Nodwell, J. R.; Willey, J. M. The SapB Morphogen Is a Lantibiotic-like Peptide Derived from the Product of the Developmental Gene RamS in Streptomyces Coelicolor. *Proc Natl Acad Sci U S A* **2004**, *101* (31), 11448–11453. https://doi.org/10.1073/pnas.0404220101.

(52) Sarksian, R.; Hegemann, J. D.; Simon, M. A.; Acedo, J. Z.; van der Donk, W. A. Unexpected Methyllanthionine Stereochemistry in the Morphogenetic Lanthipeptide SapT. *J Am Chem Soc* **2022**, *144* (14), 6373–6382. https://doi.org/10.1021/jacs.2c00517.

(53) van Gestel, J.; Vlamakis, H.; Kolter, R. Division of Labor in Biofilms: The Ecology of Cell Differentiation. *Microbiol Spectr* **2015**, *3* (2), MB-0002-2014. https://doi.org/10.1128/microbiolspec.MB-0002-2014.

(54) Arnaouteli, S.; Bamford, N. C.; Stanley-Wall, N. R.; Kovács, Á. T. Bacillus Subtilis Biofilm Formation and Social Interactions. *Nat Rev Microbiol* **2021**, *19* (9), 600–614. https://doi.org/10.1038/s41579-021-00540-9.

(55) Zhang, S.; Haldenwang, W. G. RelA Is a Component of the Nutritional Stress Activation Pathway of the Bacillus Subtilis Transcription Factor Sigma B. *J Bacteriol* **2003**, *185* (19), 5714–5721. https://doi.org/10.1128/JB.185.19.5714-5721.2003.

(56) Piskunova, J.; Maisonneuve, E.; Germain, E.; Gerdes, K.; Severinov, K. Peptide-Nucleotide Antibiotic Microcin C Is a Potent Inducer of Stringent Response and Persistence in Both Sensitive and Producing Cells. *Mol Microbiol* **2017**, *104* (3), 463–471. https://doi.org/10.1111/mmi.13640.

(57) Ababneh, Q. O.; Herman, J. K. RelA Inhibits Bacillus Subtilis Motility and Chaining. *J Bacteriol* **2015**, *197* (1), 128–137. https://doi.org/10.1128/JB.02063-14.

(58) Baba, T.; Ara, T.; Hasegawa, M.; Takai, Y.; Okumura, Y.; Baba, M.; Datsenko, K. A.; Tomita, M.; Wanner, B. L.; Mori, H. Construction of Escherichia Coli K-12 in-Frame, Single-Gene Knockout Mutants: The Keio Collection. *Mol Syst Biol* **2006**, *2*, 2006.0008. https://doi.org/10.1038/msb4100050.

(59) Yagmurov, E.; Tsibulskaya, D.; Livenskyi, A.; Serebryakova, M.; Wolf, Y. I.; Borukhov, S.; Severinov, K.; Dubiley, S. Histidine-Triad Hydrolases Provide Resistance to Peptide-Nucleotide Antibiotics. *mBio* **2020**, *11* (2). https://doi.org/10.1128/mBio.00497-20.

(60) Bantysh, O.; Serebryakova, M.; Makarova, K. S.; Dubiley, S.; Datsenko, K. A.; Severinov, K. Enzymatic Synthesis of Bioinformatically Predicted Microcin C-like Compounds Encoded by Diverse Bacteria. *mBio* **2014**, *5* (3), e01059-14. https://doi.org/10.1128/mBio.01059-14.

(61) Ho, S. N.; Hunt, H. D.; Horton, R. M.; Pullen, J. K.; Pease, L. R. Site-Directed Mutagenesis by Overlap Extension Using the Polymerase Chain Reaction. *Gene* **1989**, *77* (1), 51–59. https://doi.org/10.1016/0378-1119(89)90358-2.

(62) Pomerantsev, A. P.; Camp, A.; Leppla, S. H. A New Minimal Replicon of Bacillus Anthracis Plasmid PXO1. *J Bacteriol* **2009**, *191* (16), 5134–5146. https://doi.org/10.1128/JB.00422-09.

(63) Kitagawa, M.; Ara, T.; Arifuzzaman, M.; Ioka-Nakamichi, T.; Inamoto, E.; Toyonaga, H.; Mori, H. Complete Set of ORF Clones of Escherichia Coli ASKA Library (a Complete Set of E. Coli K-12 ORF Archive): Unique Resources for Biological Research. *DNA Res* **2005**, *12* (5), 291–299. https://doi.org/10.1093/dnares/dsi012.

(64) National Research Council. *Specifications and Criteria for Biochemical Compounds*, 3rd ed.; The National Academies Press: Washington, DC, 1972.

(65) Shemesh, M.; Chai, Y. A Combination of Glycerol and Manganese Promotes Biofilm Formation in Bacillus Subtilis via Histidine Kinase KinD Signaling. *J Bacteriol* **2013**, *195* (12), 2747–2754. https://doi.org/10.1128/JB.00028-13.

1 **TOC Graphic**

2